Climate-driven variability in *Euphausia pacifica* size distributions off northern California

Roxanne R. Robertson[a,c]

Eric P. Bjorkstedt[b,c]

[a] Cooperative Institute for Marine Ecosystems and Climate, Humboldt State University, Arcata, CA, USA

[b] NOAA Fisheries, Southwest Fisheries Science Center, Fisheries Ecology Division, Santa Cruz, CA, USA

[c] Department of Fisheries Biology, Humboldt State University, Arcata, CA, USA

Abstract

We analyzed an 11-year data set of length measurements for *Euphausia pacifica*, resolved by developmental stages ranging from early furcilia through adults, to characterize temporal variability in size distributions in relation to environmental and climate forcing in coastal waters of the northern California Current. Our analysis reveals that coastal size distributions of this linchpin species are related to temperature and chlorophyll *a* concentration, and indicate that warm climate events disrupt and suppress typical seasonal dynamics, resulting in persistent shifts towards populations dominated by smaller juveniles and adults. The 2014-16 marine heatwave (MHW) resulted in sharp and sustained transition in the size structure of *E. pacifica* off northern California; we captured numerous mature individuals smaller than any previously reported in the literature and larger size classes were conspicuously absent or rare when the MHW most strongly impacted coastal waters. Early life history stages exhibited a contrasting response, shifting instead towards larger size distributions during warm conditions. Advection appears to be the dominant mechanism driving rapid shifts in *E. pacifica* size structure off northern California, which implies alongshore and cross-shelf gradients in life history expression (e.g., changes in size-at-maturation) related primarily to temperature. Variability in food availability (chlorophyll concentration) and physiological responses (e.g., changes in growth rates) likely contribute to seasonal variability, but appear insufficient to account for sharp, climate-driven transitions. Climate-driven shifts in individual and total biomass of this critical and dominant forage species have important ecological implications, particularly for growth and survival of species at higher trophic levels. Given that warm water events are likely to increase with climate change, the effects of the 2014-16 MHW on *E. pacifica* in coastal waters may serve as a harbinger for future change. Detailed information on size structure of euphausiid populations is fundamental to understanding population responses to and ecosystem consequences of climatic and environmental forcing, and has been incorporated in assessments that support ecosystem-based approaches to fisheries management.

1. Introduction

Within the California Current Ecosystem (CCE) euphausiids, commonly known as krill, play a crucial role linking primary production to higher trophic levels, including numerous ecological and economically important organisms such as salmonids, rockfishes, seabirds, and marine mammals (Tanasichuk, 2002; Brodeur and Pearcy, 1992; Abraham and Sydeman, 2004; Becker et al., 2007; Schoenherr, 1991). Among those species that are not directly dependent on euphausiids, most are within two trophic links of them at some point in their life history (Field. et al., 2006). Changes in euphausiid populations can alter trophic pathways and ecosystem functioning, often with substantive consequences for higher trophic levels (Sydeman et al., 2006; Lindley et al., 2009; Ruzicka et al., 2012; Wells et al., 2012; Jones et al., 2018; Santora et al., 2020). Recognition of their importance to marine ecosystems and fisheries productivity motivated a pre-emptive moratorium on euphausiid harvest in the California Current and has spurred investigations focused on spatial patterns in relation to oceanographic and bathymetric structure (Gómez-Gutiérrez et al., 2005; Ressler et al., 2005; Santora et al., 2011; Santora et al., 2012; Fiechter et al., 2020) and temporal variability in response to climate forcing (Dorman et al., 2015a; Sydeman et al., 2013; Brinton and Townsend, 2003).

Several studies have documented the response of euphausiid populations to environmental and climatic variability in various regions of the CCE. Variability in the onset and intensity of upwelling affects the abundance of *Euphausia pacifica* and *Thysanoessa spinifera*, species that usually dominate under typical (relatively cool and productive) upwelling conditions (Tanasichuk, 1998; Gómez-Gutiérrez et al., 2005). Delayed onset of upwelling can affect higher trophic levels by negatively impacting euphausiid biomass (Sydeman et al., 2006, Dorman et al., 2011). El Niño events have particularly strong effects on euphausiid populations and communities throughout the CCE and regions to the north and south (Mackas and Galbraith, 2002; González et al., 2000; Brinton and Townsend, 2003). During these events, euphausiid biomass tends to decline, especially for cool water species, and warm-water species are encountered more frequently and with greater abundance (Smith, 1985; Marinovic et al., 2002; Lilly and Ohman, 2018; Bjorkstedt and Robertson, in prep.).

Population level responses to climate variability are likely to be mirrored by changes in individual characteristics related to environmental conditions that affect development and growth. Euphausiid

energetics are strongly influenced by temperature (Lasker, 1966; Fowler et al., 1971; Ross, 1981; Ross 1982a; Iguchi and Ikeda, 1995). Growth and development rates of E. *pacifica* are positively related to temperature (Ross, 1982a), yet individuals tend to mature at smaller size under warmer conditions (Ross 1982b; Forster et al., 2012). How *E. pacifica* respond to variability in prey resources is less clear. In the northern California Current, *E. pacifica* growth does not exhibit a strong relationship with chlorophyll concentration (Shaw et al., 2010), whereas tight coupling between growth and chlorophyll concentration has been observed elsewhere along the coast of North America (Pinchuk and Hopcroft, 2007; McLaskey et al., 2020). Although several studies document selectivity for diatoms and varying degrees of omnivory in *E. pacifica* (e.g., Ohman, 1984; Du and Peterson, 2014; Dilling et al., 1998), effects of food quality or diversity on euphausiid growth rates remain poorly. Complicating matters, many euphausiids, including *E. pacifica,* have the capacity to shrink during periods of starvation, bouts of intense reproductive effort, or exposure to increased temperatures (Nicol et al., 1992; Pinchuk and Hopcroft, 2007; Feinberg et al., 2007; Shaw et al., 2010; Marinovic and Mangel, 1999).

In this paper, we describe an 11-year data set of length measurements for *Euphausia pacifica*, resolved by developmental stage from early furcilia through adults, collected in coastal waters off northern California, and characterize variability in size-structure in relation to seasonal and interannual variability in temperature and chlorophyll *a* concentration. Specifically, we examine the hypothesis that *E. pacifica* tend to be larger (smaller) during cooler (warmer) conditions. This hypothesis is based on well-documented relationships between temperature and euphausiid growth and development dynamics (e.g., Ross, 1981; Ross, 1982a; Feinberg, 2006) and broad observations that indicate temperature has an important role in determining individual body size and population size distributions (e.g., Atkinson, 1994; Daufresne et al., 2009). We also examine the hypothesis that greater (lower) chlorophyll *a* concentration is related to larger (smaller) euphausiids. Including chlorophyll concentration in our analysis reflects the common observation that, all else constant, more food typically supports greater growth. We are particularly interested in the biological response to the 2014-16 marine heatwave (MHW; Hobday et al., 2018; Jacox et al., 2018a), but we also assess responses to lesser warming events (e.g., the 2009-10 El Niño) in contrast to periods marked by cooler conditions and more intense upwelling. *E. pacifica* are a dominant species in the California Current (Brinton and Wyllie, 1976; Dorman et al., 2005), therefore understanding its dynamics in the context of environmental variability is expected to yield important insight to the structure and function of the California Current Ecosystem.

1.1 Recent Climate Variability in the California Current

During the past decade the CCE experienced substantial climate variability, including record-breaking warm water anomalies. Except for a brief interruption by the moderate 2009-10 El Niño, basin scale indices reflected relatively cool and productive conditions from 2007 through 2013 (Fig. 1). During winter 2013-14 climate indices affecting the CCE underwent a major phase shift; the Pacific Decadal Oscillation (PDO), North Pacific Gyre Oscillation (NPGO), and Multivariate ENSO Index (MEI) changed phase, indicating a transition to a warmer and less productive North Pacific Ocean. Coincident with and following this climatic shift, the CCE experienced a severe and unprecedented MHW that lasted several years (2014-16) and extended throughout the entire NE Pacific (Hobday et al., 2018; Jacox et al., 2018a). In the northern portion of the California Current, the initial phase of the MHW was marked by the arrival of warm 'blob' waters in fall 2014 (Bond et al., 2015; Peterson et al., 2015). Warm water anomalies persisted into 2016 and were influenced by one of the strongest tropical El Niño events on record during 2015-16 (Gentemann et al., 2016; McPhaden, 2015; Jacox et. al, 2016). By early 2017, conditions in the central and southern CCE had returned to near normal. However, recovery from the MHW and El Niño was slower in the northern CCE, where warm water anomalies and zooplankton taxa persisted into mid-2017 (Wells et al., 2017; Bjorkstedt and Robertson, in prep.).

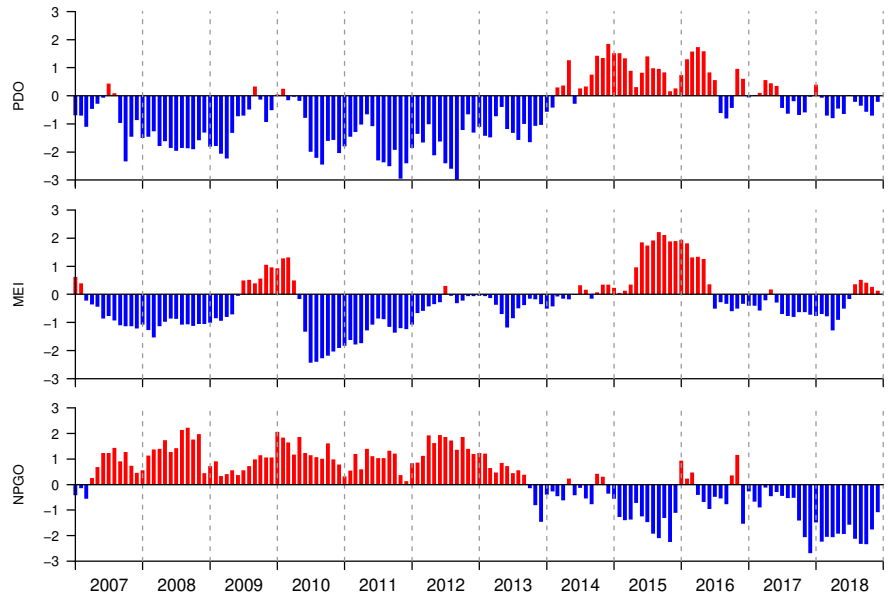

Fig. 1. Basin-scale climate indices. Panels from top to bottom: Pacific Decadal Oscillation (PDO), Multivariate Enso Index (MEI.v2) and North Pacific Gyre Oscillation (NPGO; monthly averages).

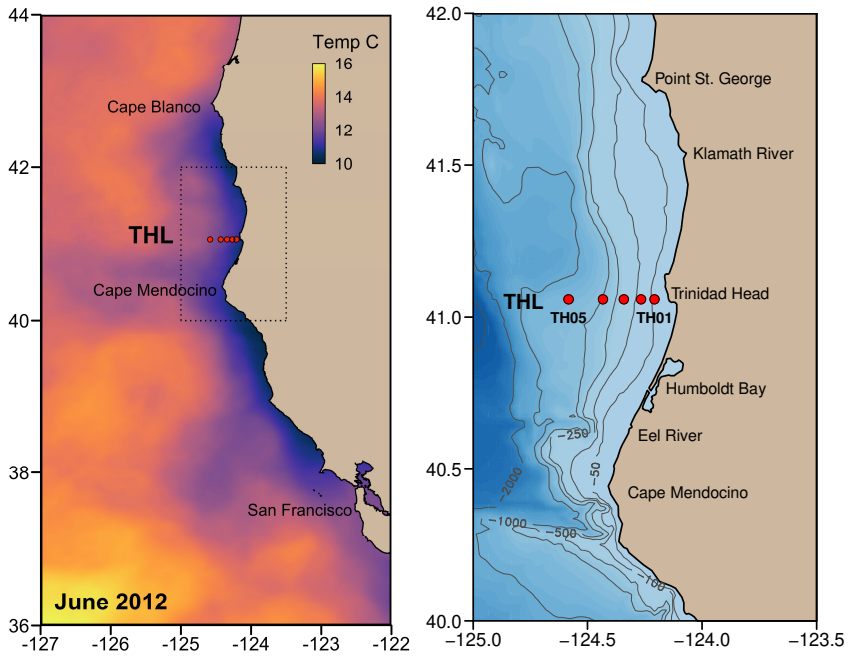

Fig. 2. Trinidad Head Line (THL) off northern California (41°03.50 N). Red points indicate THL station locations. Left panel: THL overlain on monthly composite Multi-scale Ultra-high Resolution Sea Surface Temperature (June 2012). Dotted rectangle indicates area depicted in right panel. Right panel: THL stations (TH01 – TH05) overlain on bathymetry (depth contours in meters).

1.2 Trinidad Head Line

The Trinidad Head Line (THL; 41.05° N; Fig. 2) lies in a zone of transition between the northern California Current (NCC), which is dominated by strongly seasonal upwelling and downwelling along a generally linear coast (Hickey and Banas, 2009), and regions to the south where upwelling typically is both less seasonal and more intense than in the north, and interactions between coastal topography, winds, and alongshore flow lead to greater complexity and mesoscale structure in coastal circulation (Largier et al., 1993; Batteen, 1997; Strub and James 2000). The region nominally represented by the Trinidad Head lies between Cape Blanco and Cape Mendocino, two major headlands that strongly influence coastal circulation through the generation of mesoscale upwelling jets and eddies (Hayward and Mantyla, 1990; Barth et al., 2000). Upwelling in this region is most consistent and reaches maximum intensity in the spring and summer; upwelling can occur during the late fall and winter, but is weaker, and often countered by southerly winds associated with winter storms (Leising et al., 2015). Circulation in the area north of Cape Mendocino can be relatively sluggish, even during intense upwelling, owing to the dominant winds having a substantial onshore component along the westward jutting coastline (Largier

et al., 1993; Garcia-Reyes and Largier, 2012). During winter and early spring, coastal waters are impacted by freshwater discharge from major rivers (e.g., the Klamath and Eel) and numerous smaller coastal watersheds.

2. Methods

2.1 Trinidad Head Line Sampling

Hydrographic data and plankton samples have been collected along the THL since 2007. The THL currently extends from the inner shelf to the upper slope waters (5 - 37 km offshore) and consists of five stations, three of which lie over the shelf (TH01, 35 m bottom depth; TH02, 75 m; TH03, 140 m) and two offshore of the shelf break (TH04, 460 m; TH05, 780 m) (Fig. 2). Cruises occur at roughly monthly (occasionally biweekly) intervals. Sampling is conducted during 12-hour cruises that, with few exceptions, have been scheduled to sample stations offshore of the shelf during darkness so that zooplankters exhibiting diel vertical migrations will be more susceptible to capture. Shelf stations were often occupied after sundown during the early part of the time series, but are now occupied during late afternoon to minimize navigational challenges and risk of fouling with crab gear.

2.1.1 Hydrographic Observations

At each station hydrographic data are collected with a Sea Bird Electronics (SBE) model 19 plus V2 CTD (19 plus until September 2014) cast to a maximum depth of 500 m (150 m until August 2014) or to within a few meters of the seafloor. The CTD is integrated with a SBE ECO-55 water sampler and several auxiliary sensors. The CTD and its auxiliary sensors are calibrated annually or bi-annually by Sea Bird Electronics. CTD casts and zooplankton sampling are performed almost simultaneously. Consequently, collection of hydrographic data occur during late afternoon through midnight. CTD data were initially processed using SBE Data Processing software (version 7.26.4.23) and resulting profiles were projected to 1 m depth intervals. Fluorescence data (WET Labs WET Star WS3S) were used as a proxy for chlorophyll *a* concentration. Depth-by-time Hovmöller plots displaying variability in water column structure were compiled by interpolation across the time series of hydrographic casts for individual stations.

158 **2.1.2 Zooplankton Collections and Sample Processing**

159 Zooplankton were sampled with a 0.7 m diameter Bongo sampler fitted with 505 and 335 µm mesh that
160 has been dyed dark purple and flowmeters (General Oceanics). At each station, the net was deployed
161 rapidly to a maximum depth of 100 m (or within a few meters of the sea floor) and subsequently
162 retrieved along an oblique profile by maintaining a steady wire retrieval rate (20 m min^{-1}) and adjusting
163 ship speed through the water to maintain a wire angle of 45°(± 5°) throughout the tow. Nets were
164 gently and thoroughly washed down to concentrate retained plankton in the cod-end and samples were
165 immediately transferred to sample jar(s) for preservation. For this paper, we analyze samples collected
166 with the 505 µm mesh net, and preserved in 5% formalin buffered with a saturated solution of sodium
167 borate in seawater.
168
169 In the laboratory, samples were temporarily transferred to fresh water and quantitatively fractioned
170 with a 1.25L Motodo box plankton splitter (Aquatic Sciences) to produce tractable subsamples for
171 analysis. When samples were split, subsamples consisted of at least 100 euphausiids. Euphausiids were
172 removed under magnification, and subsequently identified to species and stage, and for adults,
173 distinguished by sex. Taxonomic identification was corroborated with online sources (Brinton et al.,
174 1999). Stage designations were determined independently of length by examination of morphological
175 features indicative of developmental stage, again supported by comparison to published descriptions.
176 Specifically, adult euphausiids were distinguished from juveniles on the basis of whether an individual
177 exhibited male or female sexual characteristics, not a critical size threshold. Because *E. pacifica* F4 and
178 F5 furcilia cannot be distinguished based on telson spines, these stages were combined and treated as
179 one stage. For each species-stage combination that occurred in a sample, body length (BL) of up to 25
180 individuals were measured in millimeters from the back of the eye to base of the telson (Shaw et al.,
181 2010). Larger individuals were measured using the microscope's ocular micrometer. Smaller specimens
182 (< 5 mm) were measured from images captured with a Luminera camera (Infinity 2). Both ocular
183 micrometer and digital measurement were regularly calibrated with a stage micrometer.
184
185 **2.2 Local Oceanographic Conditions (MURS and CUTI)**

186 As indices of regional oceanographic conditions, we obtained monthly sea surface temperatures (SSTs)
187 and temperature anomalies derived from the Jet Propulsion Laboratory's (JPL) Multi-scale Ultra-high
188 Resolution (MUR) SST Analysis (JPL MUR MEaSUREs Project., 2010) for 2007-2018 for a grid cell centered
189 at 41.05° N and 125.00° W (https://coastwatch.pfeg.noaa.gov/erddap/griddap/jplMURSST41mday.html;

https://coastwatch.pfeg.noaa.gov/erddap/griddap/jplMURSST41anommday.html). Monthly anomalies are a mean of the daily anomaly product for a given month. Daily anomalies are produced by the Environmental Research Division (ERD)as deviations from a climatology based on the source data (2003-2014). We also obtained daily and monthly values of the Coastal Upwelling Transport Index (CUTI; Jacox et al., 2018b) for 2007-2018 for a grid cell centered at 41° N (accessed 1 June 2019, http://www.mjacox.com/wp-content/uploads/2019/06/CUTI_monthly.csv). Cumulative CUTI was calculated using daily CUTI values from January 1 through December 31.

2.3 Data processing and statistical analysis

All data analysis was conducted in R (version 3.5.1; R Core Team, 2018).

Preliminary inspection of the data indicated that variability in abundance and size-distribution were generally coherent across the transect, especially across station where a particular life history stage was consistently present at high density (Fig. 4). Therefore, except where noted, we present results from analysis of data aggregated by cruise. This resolution is expected to effectively capture responses to climate forcing, while minimizing the influence of covariation among stations within a cruise and among individuals within a station on statistical significance of fitted models. General patterns emerging from our analysis at the resolution of cruises were corroborated by analysis of data aggregated at different temporal resolutions (e.g., by year) or analysis at the scale of individual stations.

For each life history stage (LHS), we estimated mean length, weighted by areal density at each station. Areal density (N m^{-2}) was estimated by expanding the number of individuals identified to account for the fraction of the total sample analyzed, the volume of water filtered, and the depth of the sampled water column. We also developed density-weighted, cruise-specific length distributions. For adult and juvenile life history stages, we characterized multi-modal length distributions (when apparent) by binning size distributions into 1 mm size classes and implementing Hasselblad's (1966) steepest-descent algorithm.

To assess coherence in size variability across LHS, we estimated correlations in mean length among LHS within cruises using function 'ccf' and 'cor' in package 'corrplot' (version 0.84; Wei et al., 2017). Preliminary examination indicated that correlations among stages tended to be strongest for concurrent measurements (data not shown).

Based on the uneven spacing of our observations over time, the extent of some gaps (> 2 months in some cases), and a reluctance to obscure variability at short time scales, we elected to analyze data in its original temporal structure rather than to aggregate or interpolate data to evenly spaced time intervals. We examined temporal variability in environmental conditions and mean length at seasonal and interannual time scales. At the seasonal scale, we describe a seasonal climatology for mean cruise temperature, mean cruise $\log_{10}$(chlorophyll a + 1), and mean stage-specific length by fitting generalized additive models (GAMs) for each response variable as a function of day of year. GAMs were based on a cyclic cubic spline to favor continuity across the start and end of the annual seasonal cycle. To resolve interannual variability, we fit GAMs for mean environmental conditions and mean length on cruise date. The number of distinct piecewise smooths in the time series GAM was selected by visual inspection to ensure that the fitted curve captured low-frequency variability and lacked substantial excursions from trends in mean length over time. GAMs were fit using functions in package 'mgcv' (Wood, 2017).

To examine stage-specific relationships between *E. pacifica* length and environmental conditions, we fit linear mixed effects (LME) models, in which the potential for random variability in the slope and intercept of length-environment relationships associated with (calendar) year was assessed, and if present accounted for. Models were fit to relate mean length to temperature and chlorophyll *a* concentration (based on raw fluorescence) averaged over the sampled (max 100 m) water column across the transect. Chlorophyll concentrations were $\log_{10}$(n+1) transformed prior to averaging. Based on preliminary examination of the data, we considered models that allowed the relationship between length and temperature to vary with year and included chlorophyll concentration as a covariate with effects independent of temperature.

Optimal model structure, in terms of random and fixed effects, was identified following protocols outlined in Zuur et al. (2009), and using Akaike's Information Criterion corrected for small sample size ('AICc' in 'MuMIn' package, version 1.43.6; Bartoń, 2019) and likelihood-ratio tests ('anova'; R Core Team, 2018) to inform model selection. Models were fit using functions in 'nlme' (version 3.1-137; Pinheiro et al., 2018). Collinearity was assessed and optimal models were validated by graphical evaluation of assumptions (Zuur, 2010). Results from this analysis proved insensitive to the extent of the upper water column selected or to minor adjustments to the stations included in the spatial average of environmental conditions.

To support interpretation of results from LME models, we generated metrics that express percent change in euphausiid body length associated with change in temperature (dT) and chlorophyll concentration (dC) for an individual of mean length for each LHS at mean temperature and mean chlorophyll. dT scales the slope of the fixed effect of temperature by mean length as a general indicator of percent change in length associated with a change in temperature of 1°C. dC scales the slope of the fixed effect of chlorophyll concentration by the mean length*0.1 as an indicator of percent change in length with a change of 0.1 in $\log_{10}$([chl *a*]+1). We also calculated a metric to capture the range of variability arising from year-to-year variability in the length-temperature relationship (rYT). This metric expresses the range of expected length across years (excluding 2010 due to incomplete seasonal coverage) as a percentage relative to mean length at mean temperature and mean chlorophyll. Positive (negative) rYT indicates larger size during warm (cool) years.

To complement results emerging from analyses based on mean length and mean environmental conditions, we applied canonical correspondence analysis (CCA) using function 'cca' in package 'vegan' (version 2.5-5; Oksanen et al., 2013) to assess correlation between water column structure and adult size distributions at the scale of individual samples. For each sample, we binned *E. pacifica* adult lengths into 1 mm size classes to generate a station-by-size class matrix. A corresponding temperature-by-station matrix was created by binning temperature in the upper 100 m of the water column to 0.25°C intervals and quantifying the vertical extent (at 1 m resolution) of the water column in each temperature bin. CCA was applied to estimate the strength and structure correlation between the resulting size and temperature matrices. Statistical significance was assessed with a permutation test using function 'anova.cca' in package 'vegan' (n = 10,000).

We calculated individual biomass by first converting body length (BL; mm) to total length (TL; mm) and subsequently calculating dry weight (DW, µg) and biomass (B; µgC) per the following relationships

$$TL = 1.218*BL + 0.2807$$

$$DW = 0.795*TL^{3.239}$$

$$B = -1.985 + 0.401*DW$$

following (Shaw et al., 2010; Feinberg et al., 2007; Ross, 1982a). Biomass (divided by 1000) was then expanded to areal density (mgC m^{-2}) by summing over size-distributions and applying cruise-specific density estimates.

3. Results

Our data set includes measurements of over 30,000 individual *E. pacifica,* spanning F1 – F7 furcilia, juvenile, and adult life history stages (Table 1) from the five core stations (TH01-TH05) over the course of 119 cruises conducted between November 2007 and December 2018 and associated hydrographic data. *E. pacifica* represent approximately 80% (by numerical density) of the euphausiid assemblage along the THL. The data set includes observations from a handful of cruises that were cut short by deteriorating weather, so that only three or four stations were occupied. Four cruises were conducted on an unusual schedule so that offshore stations were collected during daylight hours. We exclude data from these cruises in statistical analyses as preliminary examination of these data suggested a strong day-night bias in abundance, presumably related to well-documented diel vertical migration behaviors (Brinton, 1965; Brinton and Townsend, 2003). We lack samples from cruises during summer 2010 due to the loss-at-sea of our Bongo net.

	This study		Boden (1950)	Ross (1981)		Feinberg et al. (2006)		Ross (1981)	
				8°C		**10.5°C**		**12°C**	
Stage	Range of Mean Length	Range of Mean Biomass	Range of Length	Development Time	Duration	Development Time	Duration	Development Time	Duration
Ad	8.46 - 17.27	662 - 6412	*8.75 - 17.78	--	--	--	--	--	--
Jv	3.98 - 11.06	62 - 1549	*4.65 - 7.93	68	--	58.4	--	45	--
F7	3.40 - 5.79	37 - 200	4.07 - 5.06	60	8	55.4	3	40	5
F6	3.25 - 4.53	32 - 93	3.82 - 4.65	55	5	51	4.4	36.5	3.5
F4/5	2.93 - 4.34	23 - 81	3.17 - 4.23	50	5	43.4	7.6	33	3.5
F3	2.57 - 3.62	15 - 46	2.67 - 3.99	38.5	11.5	32.4	11	27.5	5.5
F2	2.19 - 3.44	9 - 39	2.59 - 3.09	31	7.5	26.7	5.7	23	4.5
F1	1.53 - 2.93	2 - 23	2.18 - 2.35	22	9	21.3	5.4	17.5	5.5

Adult lifespan: 1+ years (Ross, 1982; Feinberg et al., 2006); * from Brinton and Wyllie, 1976

Table 1. Stage-specific range of mean lengths (mm) and biomass (μg C ind^{-1}) of *Euphausia pacifica* adults (Ad), juveniles (Jv), and F7 – F1 furcilia measured in this study and in Boden (1950) and Brinton and Wyllie (1976). Median development time (days to stage) and stage duration (days) at 8, 10.5, and 12 °C (from Ross, 1981 and Feinberg et al., 2006) provided as context for interpretation of results.

3.1 Local Oceanographic Conditions

A comprehensive analysis of variability in hydrographic structure along the Trinidad Head Line is beyond the scope of this paper and will be developed elsewhere. For the present analysis, we describe hydrographic conditions at the outer-shelf station (TH03; Fig. 2) as representative of the state of the ocean along the Trinidad Head Line. Observations at this station (and elsewhere along the transect) capture annual transitions between seasonal upwelling and downwelling, including variability in the

timing of these transitions, as well as the local signature of larger scale processes captured in basin-scale oceanographic climate indices spanning the THL record (Fig. 3).

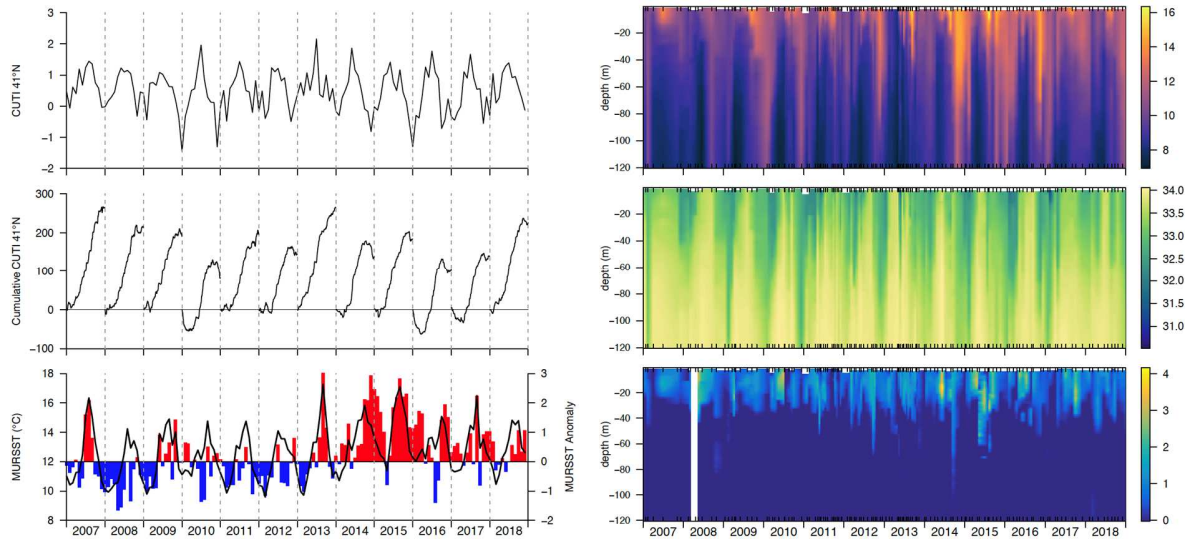

Fig. 3. Local oceanographic conditions and hydrography along the THL. Left panel from top to bottom: monthly average coastal upwelling transport index (CUTI; m^2s^{-1}) at 41°N; cumulative CUTI (calculated from daily CUTI at 41°N from Jan. 1 to Dec.31); MURS monthly sea surface temperature (°C; black line) and SST anomaly (red and blue bars) at 41.05°N, 125°W (see section 2.2 for description of anomaly product). Right panel: Hydrography along the THL as represented by station TH03 (41°03.50 N, 124°20.50 W, 140m). From top to bottom: Temperature (°C), salinity (PSU), and log chlorophyll a concentration (mg m^{-3}) by depth (m; y-axis) and time (x-axis).

Several features of the THL hydrographic record and local oceanographic conditions warrant attention as important context for interpreting variability in euphausiid length over time (Fig. 3). Conditions along the Trinidad Head Line were unusually cool during the short period of record prior to the 2009-10 El Niño. Although moderate in strength, the 2009-10 El Niño caused warming and freshening over much of the water column in response to changes in wind forcing (Fig. 3). Following the 2009-10 El Niño, the MEI transitioned to La Niña conditions (2010-2012; Fig. 1). Along the THL, this period was generally characterized by the juxtaposition of cool spring conditions driven by strong upwelling followed by rapid warming and freshening of the upper water column as wind forcing weakened. A minor shift to positive MEI during 2012 manifested locally in delayed and weak upwelling. Additionally, strong downwelling in spring 2012 resulted in relatively fresh water and low chlorophyll values along the THL (Fig. 3). The first phase of the 2014-16 MHW was marked by the arrival of the warm 'blob' in coastal waters (Bond et al., 2015; Chao et al., 2017) and the rapid development of strong warming extending to at least 60 m depth.

This transition, although appreciable, was preceded by surface warming in 2013, during which, intense spring upwelling gave way to the strongest surface temperature anomaly in the recent local record (Gentemann et al., 2016), and early 2014 when unusually warm conditions were observed in advance of the more extensive (deeper) warm 'blob' signal (Leising et al., 2015). Following a brief period of upwelling-driven cooling in early 2015, weak upwelling followed by sustained downwelling and poleward flow associated with the strong 2015-16 El Niño influenced warm water anomalies; winter and spring temperatures remained at least 1°C warmer than average at the surface and had a strong, persistent signature in the upper 60-70 m of the water column (Fig. 3). Warm conditions persisted into late 2016 and early 2017, but by late 2017 and into 2018 unusually warm conditions were again restricted to the upper water column. Warm water anomalies abated further during winter 2018, as relatively weak storm activity and downwelling allowed relatively cool, salty waters to persist over the shelf.

3.2 Cross-shelf patterns in stage-specific distributions and size structure

Stage-specific cross-shelf distributions of *E. pacifica* exhibited a consistent ontogenetic pattern marked by a shift from the broad dispersion of early furcilia stages (F1 and F2) across the transect towards the more concentrated distribution of adults and juveniles over the outer shelf and offshore of the shelf break (Fig. 4). Stage-specific size distributions of immature life history stages were generally consistent across the transect in aggregate (Fig. 4) and within cruises (correlations of mean size among stations across the time series ranged from 0.71 to 0.99, yielding slope estimates of 0.74 to 1.16 from linear models forced through the origin (data not shown). Size distributions of adult *E. pacifica* were consistent at offshore stations where adults were most abundant. The few adult *E. pacifica* captured at inshore stations are an exception to this pattern, as these individuals tended to be larger than those captured further offshore. Adult length distributions frequently included two or more distinct modes. When this occurred, further inspection indicated that these modes were in general consistently represented across stations and did not arise from aggregation of spatially distinct modes in the size distribution. In general, stage-specific size distributions overlapped, but mean size consistently differed across stages over time.

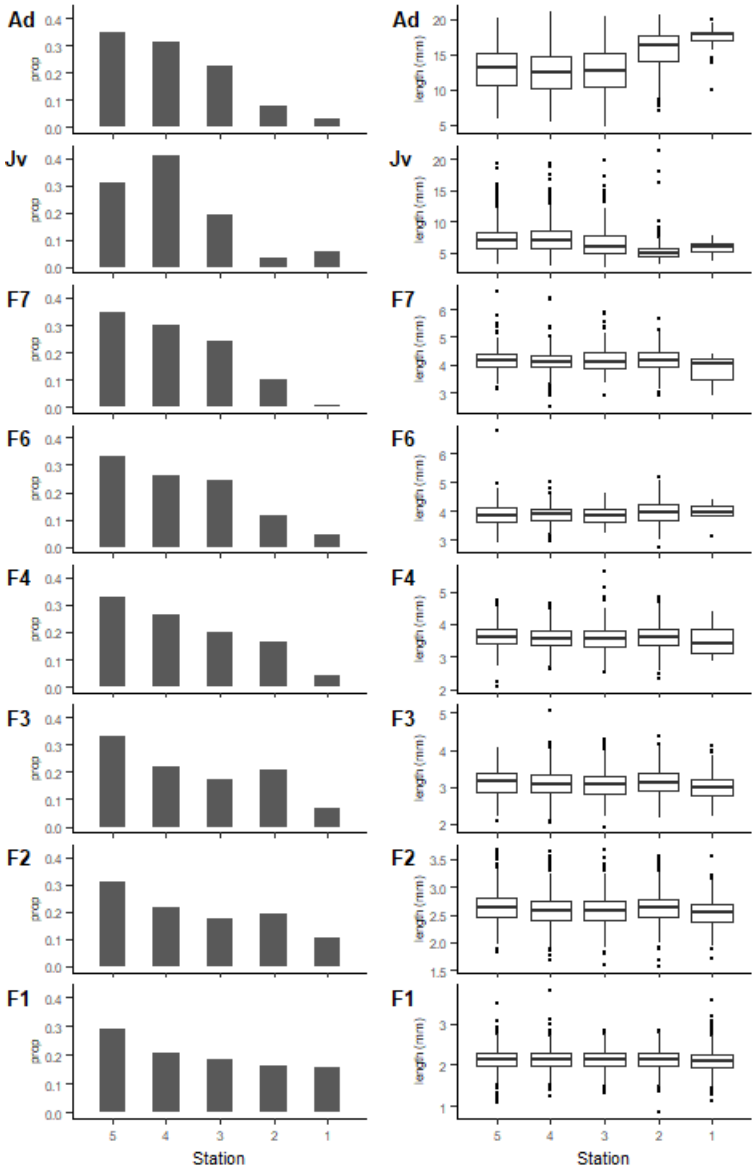

Fig. 4. Stage-specific cross-shelf distributions (left-hand column) and size-distributions (right-hand column) of *Euphausia pacifica* aggregated over all cruises. From top to bottom: adults (Ad), juveniles (Jv) and F7-F1 furcilia stages. Cross-shelf distributions are represented as relative abundance (y-axis) based on areal density (N m^{-2}) at stations (x-axis) TH05 (offshore) – TH01 (nearshore). Box represents the interquartile range (IQR) bounded by the 25th and 75th quartiles. Whiskers extend 1.5 IQR from the median.

3.3 Coherence in Stage-Specific Length Distributions

Mean length of adult males and females was significantly correlated ($r^2 = 0.90$, $p < 0.001$; Fig. A.1).

We observed substantial overlap between stage-specific size distributions (Fig. 4 and Table 1), yet differences in mean size across stages (including males and females) was maintained over time. Mean length of juveniles and adults was significantly correlated (r^2 = 0.34, p-value < 0.001; Table 2), as were mean lengths across furcilia stages (Table 2).

3.3.2 Furcilia

Mean length was positively correlated among all furcilia stages (r^2 = 0.23 – 0.72; p < 0.05 – 0.001; Table 2), and correlations tended to be strongest across sequential stages. Among furcilia stages, only F1 showed a significant correlation in mean size with adults (Table 2).

Stage	A	J	F7	F6	F4/5	F3	F2	F1
A		0.34***	-0.08	0.08	-0.01	0.06	0.13	0.23*
J	0.54		-0.11	-0.03	-0.11	-0.09	-0.10	0.13
F7	-0.45	-0.41		0.62***	0.56***	0.55***	0.23*	0.41***
F6	0.60	-0.13	0.72		0.68***	0.55***	0.26*	0.41***
F4/5	-0.04	-0.47	0.67	0.62		0.72***	0.30**	0.43***
F3	0.55	-0.54	0.84	0.65	0.95		0.42***	0.52***
F2	1.34	-0.54	0.37	0.31	0.42	0.43		0.38***
F1	0.02	0.02	0.21	0.27	0.27	0.43	0.33	

Table 2. Correlations (top panel) and slope estimates (bottom panel) of *Euphausia pacifica* mean body length by cruise among life history stages (furcilia F1-F7, J = juveniles, A = adults). Slopes were estimated from linear models of mean length for younger stages on older stage (e.g., F1 regressed on F2). Significance of correlation: * p < 0.05, ** p < 0.01, *** p < 0.001.

3.4 Temporal variability in stage-specific size distributions

In the following sections, we describe temporal variability in stage-specific size distributions at seasonal and interannual scales in the context of corresponding variability in temperature and $\log_{10}(n+1)$-transformed chlorophyll *a* concentration, averaged over stations and depths within a cruise.

3.4.1 Seasonal patterns

Seasonal climatology of mean temperature conformed to characteristic patterns of cooling during spring and summer associated with upwelling and equatorward transport and warming during fall and winter

(Fig. 5). This pattern held for temperature during years influenced by warming events, during which much of the divergence in temperature from climatological conditions occurred during fall and winter. Winter temperatures remained low during winter under cool climate conditions, with intense upwelling-driven cooling noted only during spring 2013.

Chlorophyll *a* concentration also exhibits a generally consistent seasonal pattern, with seasonal maxima occurring during the summer months (Fig. 5). Substantial blooms occurred during spring and summer in both cool and warm years.

3.4.1.1 Adults and Juveniles

Adult *E. pacifica* captured along the THL tended to be larger during summer and smaller during winter across all years (Fig. 5). Seasonal (climatological) variability in adult size was more strongly (inversely) coherent with seasonal patterns in mean temperature than with climatological chlorophyll *a* concentration. Offsets from the mean seasonal pattern were linked to interannual climate variability: mean size tended to exceed seasonal means throughout the year during cool conditions, and conversely, to be smaller than expected throughout the year during warm events, and in particular during the 2014-2016 MHW.

We did not observe a consistent seasonal pattern in mean size of juvenile *E. pacifica*. Rather, the timing of seasonal maxima and minima varied substantially across years (Fig. 5). As observed for adults, however, juvenile *E. pacifica* tended to be smaller than average throughout warm years and larger during cool years.

3.4.1.2 Furcilia

Intermediate furcilia stages exhibited an opposite pattern with respect to the offset between mean size and seasonal variability in size: individuals tended to be larger under warmer than usual conditions and smaller during cool years (Fig. 5). Seasonal trends in mean size of these stages tend to lag temperature climatology and to overlap more with the seasonal pattern in chlorophyll *a* concentration. The earliest furcilia stage, F1, did not exhibit consistent offsets from seasonal mean size in relation to climate variability.

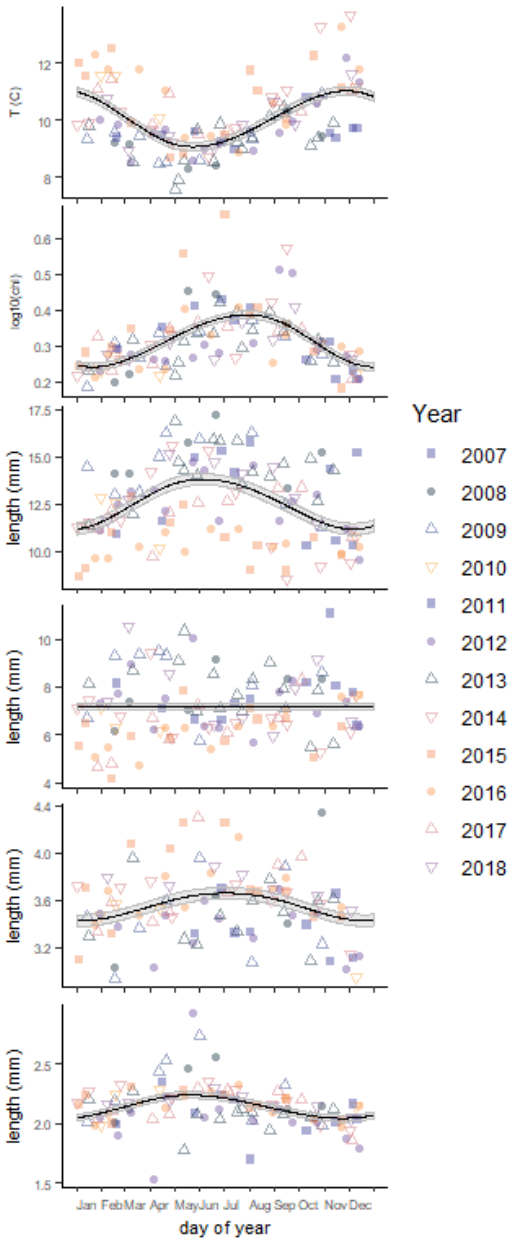

Fig. 5. Intra-annual variability in environmental conditions and *E. pacifica* length. From top to bottom: temperature (°C), $\log_{10}([\text{chl } a] + 1)$, adult, juvenile, F4/5 furcilia, and F1 furcilia length distribution (y-axis) by day of year (x-axis). Black line (±SE in grey) represents generalized additive model fit to environmental or size distribution data (see legend for year specific symbols).

3.4.2 Interannual trends

Interannual variability in mean temperature is entirely consistent with patterns described above (3.1 Local Oceanographic Conditions), with clear indication of sustained warming associated with the 2009-10 El Niño and the 2014-16 MHW, and cool periods during the early part of the record (late 2007-2009) and 2011 through mid-2014 (Fig. 6).

Low-frequency variability in chlorophyll *a* concentration was most apparent in the magnitude of seasonal maxima (Fig. 6). Several substantial blooms were observed over the course of the time series, often coinciding with (or closely following) evidence of relaxation from upwelling. Chlorophyll *a* concentration remained low during years directly influenced by El Niño events (2010 and 2016) or reduced upwelling (2017).

3.4.2.1 Adults and Juveniles

The pattern of low-frequency variability in mean length of adult *E. pacifica* is very nearly inverse that observed for mean temperature (Fig. 6). From 2007 to mid-2009, under consistently cool conditions, large (>15 mm) adults were present year-round and dominated the population. In mid-2009, as the 2009-10 El Niño began to influence the region, the size structure of the population shifted; large euphausiids were present but smaller (<10 mm) adults made up a substantial fraction of the population. Although we lack data to characterize any trends in size during the summer 2010, the tendency for small (<10 mm) and large (>15 mm) size classes to be simultaneously present year-round continued into 2011 and on through the first half of 2014. During this period, large adults tended to be dominant during summer months while small adults were more abundant in winter. One exception to this pattern occurred in 2012, when the maximum size of adults was lower and modal structure of the size distribution were less distinct. Mean adult length declined sharply with the arrival of warm 'blob' waters in mid-2014, individuals larger than 12 mm effectively disappeared from our samples. Larger adults (> 15 mm) were briefly abundant during a period of intense upwelling in early 2015, but again disappeared as the 2015-16 El Niño renewed unusually warm conditions along the coast. During this period, the typical seasonal pattern of increasing adult size during spring and summer was diminished in scope, such that mean adult length remained at or below the time series mean (12.9 mm ± 3.03 SD) and on several occasions was as low as 60-70% of the time series mean. Beginning in 2017, large (>15 mm) adults were again present in substantial numbers, and the lower bound of adult sizes increased. However, the upper range and mean adult size distributions had not yet recovered to values observed prior to 2014.

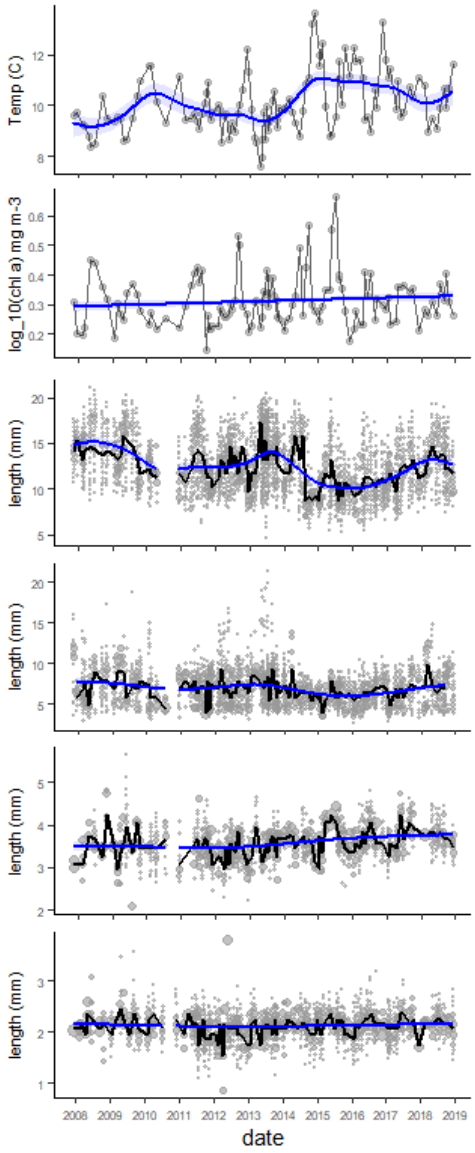

Fig. 6. Interannual variability in environmental conditions and *E. pacifica* length distributions. From top to bottom: temperature (°C), $\log_{10}$([chl *a*]+1), adult, juvenile, F4/5 furcilia, and F1 furcilia length distribution based on body length measurements (mm; y-axis) by cruise date (x-axis). Black line tracks mean length by cruise. Blue line indicates fit of generalized additive model (tuned to capture interannual trends) fit to mean of cruise-specific length distributions (gray points scale with stage-specific log-transformed density; N m^{-2}).

434

435 Low-frequency variability in juvenile length generally corresponds to patterns observed for adults (Fig.

436 6). However, the decline in juvenile size begins in late-2013, prior to the sharp decline in adult mean

length. The few unusually large juveniles detected in our samples were all captured in 2013 or during the cool years preceding the 2009-10 El Niño.

3.4.2.2 Furcilia

Greater cruise-to-cruise variability in size distributions for furcilia limited our ability to characterize low-frequency trends; most fitted GAMs indicated a slow increase in size over time, sometimes marked by a subtle inflection coincident with the onset of the 2014-2016 MHW (Fig. 6). These patterns corroborate evidence from visual inspection and comparison of seasonal patterns that furcilia tended to be smaller for a given stage during cool years and larger during periods that span or follow the warm water anomalies (2014 through 2017). Although small in absolute terms, the observed changes in mean length represent sustained shifts on the order of 5-8% across periods.

3.5 Length-Environment Relationships

3.5.1 Linear Mixed Effects Models

All life history stages exhibited a decline in mean length with increasing temperature, and for most life history stages this relationship proved to be statistically significant (Table 3). Scaled to stage-specific mean lengths, size-temperature slopes translate to reductions in length on the order of 1.09-5.68% $°C^{-1}$ for immature life history stages and 7.5% $°C^{-1}$ for adults. For most life history stages, this pattern is associated with seasonal variability: individuals tended to be smaller during warmer (non-upwelling) seasons, and conversely, larger individuals were captured during cooler (upwelling) seasons (Table 3 and Fig. 7; see Fig. A.2 for comprehensive LHS models).

For most life history stages, the optimal LME model included year-to-year random variability in the intercept of the length-temperature relationship, corresponding to an annual offset of the seasonal pattern (Table A.1).

The pattern is more complex for adults, for which the optimal model included random variation in both intercept and slope of the length-temperature relationship (Table 3). In this case, year-to-year variability captured a clear shift from steeply sloped responses (with correspondingly higher intercepts) occurring during cool years to length-temperature relationships with shallower slopes and lower intercepts during warm years, such that mean length appears to converge on a common range of smaller sizes with increasing temperature (Fig. 7). The optimal model for variation in the upper bound of adult size

stage	Fixed								Full	
	ΔAICc			slope (SE)						
(random structure)	**L ~ T + log$_{10}$ (C+1)**	L ~ T	L ~ log$_{10}$ (C +1)	T	log$_{10}$ (C + 1)	r2	dT	dC	r2	rYT
Adult (rSI)	**0**	0.77		-0.97 (0.17) ***	2.97 (1.62)	0.34	-7.50	2.29	0.62	-22.02
Juvenile (rI)	**2.16**	0		-0.39 (0.11) ***	-0.19 (1.40)	0.12	-5.68	-0.28	0.21	-11.51
F7 (rI)	**0**	2.32		-0.09 (0.03) **	0.88 (0.42) *	0.16	-2.24	2.12	0.18	1.51
F6 (rI)	**1.13**		0	-0.03 (0.03)	0.96 (0.33) **	0.12	-0.68	2.46	0.11	0.02
F4/5 (rI)	**0**			-0.08 (0.03) **	1.06 (0.32) **	0.20	-2.29	2.94	0.44	9.61
F3 (rI)	**0**			-0.07 (0.02) ***	0.56 (024) *	0.17	-2.30	1.82	0.49	13.72
F2 (rI)	**0.3**		0	-0.03 (0.02)	0.64 (0.35) *	0.11	-1.09	2.59	0.20	5.28
F1 (rI)	**0.86**	0		-0.08 (0.02) ***	0.22 (0.19)	0.24	-3.60	1.04	0.38	6.95
A_{10} (rSI)	**2.25**	0		-0.75 (0.19) ***	-0.20 (1.71)	0.19	-5.04	-0.14	0.53	-30.40
A_{90} (rI)	**0**	4.97		-1.01 (0.16) ***	5.40 (1.94) **	0.36	-10.16	5.44	0.50	-16.27

Table 3. Summary of stage-specific relationships between mean length and temperature and $\log_{10}$(n + 1)-transformed chlorophyll as characterized by linear (Fixed) and linear mixed-effects (Full) models with year as a random effect on intercept (random structure = rI) or slope and intercept (rSI). ΔAICc values shown for models with various fixed structures. Slope and standard error (SE) of coefficients for model with both environmental covariates (L ~ T + $\log_{10}$ ([chl *a*])) shown. Asterisks included in slope estimates indicate level of significance (* < 0.05, ** < 0.01, *** < 0.001). r^2 values under 'fixed' and 'full' indicate variance explained by the fixed effect of T + $\log_{10}$ ([chl *a*]+1) and by the full LME model, respectively. dT scales the slope of the fixed model by the mean length as a general indicator of percent change in length associated with a change in temperature of 1°C. dC scales the slope of the fixed model by the mean length*0.1 as an indicator of percent change in length with a change of 0.1 in $\log_{10}$([chl *a*]+1). rYT represents the range of difference in lengths across years as a percentage relative to mean length at mean(T) and mean(C). Grey cells indicate models did not have substantial support. A_{10} and A_{90} stage represent lower (10^{th} quantile) and upper (90^{th} quantile) bounds of adult size distributions, respectively.

distributions (using the 90^{th} quantile as a robust metric) indicates a strong correlation with temperature, with year-to-year offsets from common slope (Table 3 and Fig. 8). In contrast, the optimal model for variation in the lower bound of adult size distributions (10^{th} quantile) includes year-to-year variability in both slope and intercept of the length-temperature relationship, and exhibits a pattern of steeper slopes during cool years and shallower (even positive) slopes during warm years similar to that observed for variability in mean adult size.

With the exception of the juvenile and F1 stages, all life history stages exhibited positive relationships between mean length and ($\log_{10}$(n+1)-transformed) chlorophyll, and in many cases, model selection gave preference to models that included both temperature and chlorophyll *a* as explanatory variables (Table 3). Statistically significant length-chlorophyll relationships were detected only for furcilia stages (excepting F1). For two furcilia stages (F2 and F6), a model relating mean size to chlorophyll

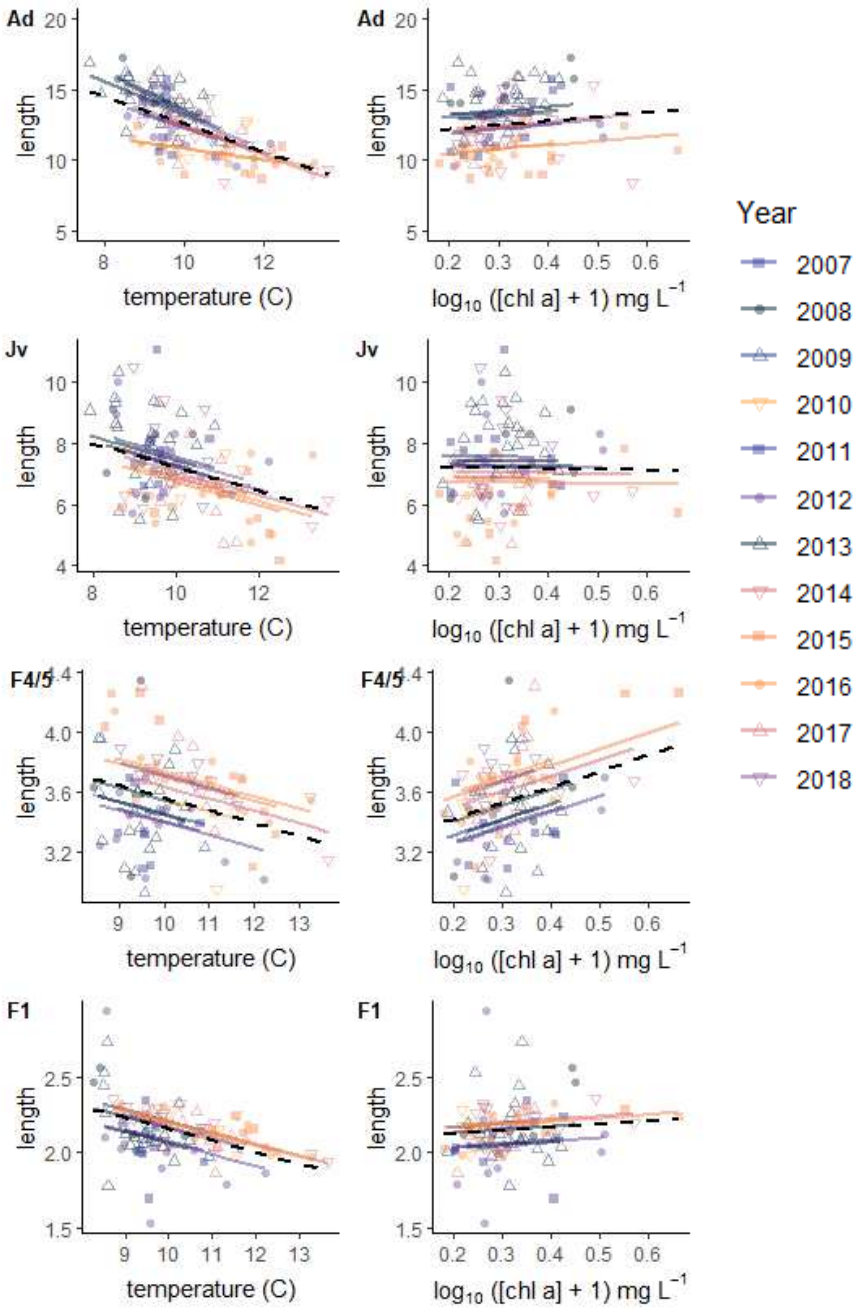

Fig. 7. Linear mixed effects models fit to stage-specific mean body length (mm; y-axis) of *Euphausia pacifica* and temperature (left; °C; 1:100m) and $\log_{10}$ ([chl *a*] + 1) (right), by year (colored lines; see legend). Black dashed-line represents fixed effect. Life history stages from top to bottom: adults (Ad), juveniles (Jv), F4/5 and F1 furcilia). Note that for display of temperature response, $\log_{10}$([chl *a*]+1) is fixed at 0.31. For display of chlorophyll response, temperature is fixed at 10°C but the random effect year on temperature has been retained to place effect of chlorophyll on length in context.

481 concentration was identified as being most parsimonious; in both cases, a model that also included
482 temperature had substantial support (ΔAICc of 0.30 and 1.13 for F2 and F6, respectively; Table 3). For F1

furcilia, chlorophyll was excluded from the best model (based on temperature), but retained in a robust alternative model (ΔAICc = 0.86; Table 3).

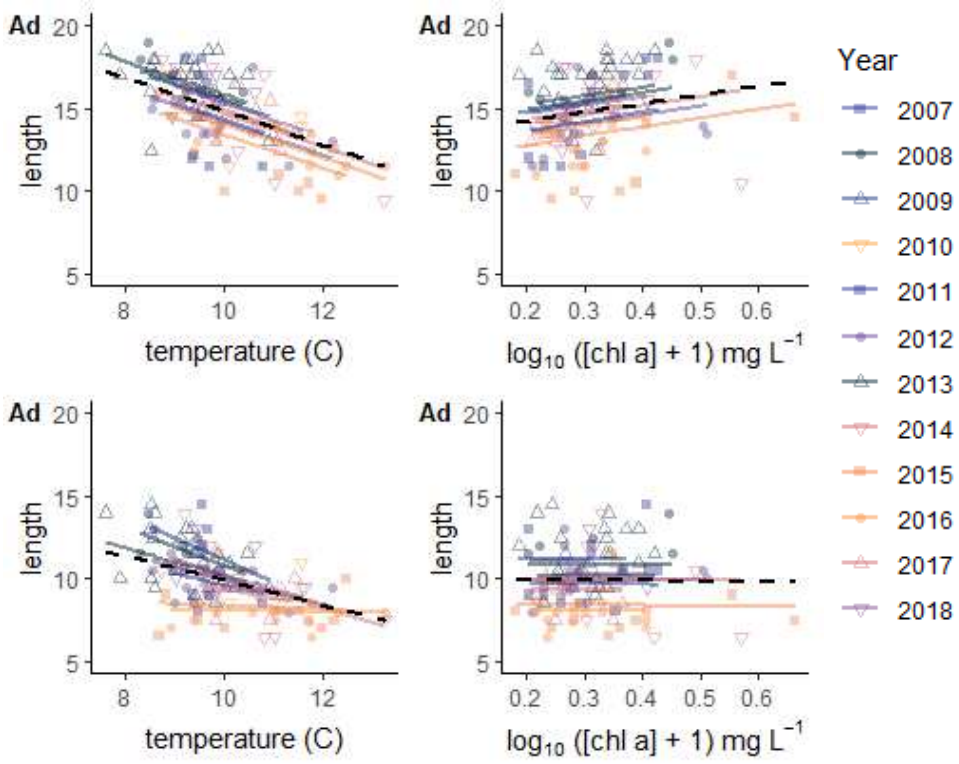

Fig. 8. Linear mixed effects models fit to upper (top plots; 90th quantile) and lower bound (bottom plots;10th quantile) adult mean body length (mm; y-axis) of *Euphausia pacifica* and temperature (left; °C; 1:100m) and $\log_{10}$([chl *a*]+ 1)(right), by year (colored lines; see legend). Black dashed-line represents fixed effect. Note that for display of temperature response, $\log_{10}$([chl *a*]+1) is fixed at 0.31.. For display of chlorophyll response, temperature is fixed at 10°C but the random effect year on temperature has been retained to place effect of chlorophyll on length in context.

3.5.2 Canonical Correspondence Analysis

Size distributions of adult *E. pacifica* were strongly correlated with water column structure (Fig. 9, $p < 0.01$), with small- to large- size classes of adult *E. pacifica* mapping neatly onto the relative proportion of the sampled water column occupied by warm to cold waters, respectively. For example, 16-17 mm adults are strongly associated with the presence of 7-8°C water, while 9-10 mm adults co-occur (in time) with waters from 13-16°C. The presence of 12-13 mm adults typically coincides with the presence of 10°C water, regardless of whether, for a particular cruise, 10°C water is relatively cold and deep and 12-13 mm adult euphausiids are among the largest present, or the converse, that 10°C water is relatively

warm and near the surface and 12-13 mm adults are on the small side. Approximately 49% of the variability in size distributions can be attributed to water column structure through this analysis, with the first two axes (eigenvectors) accounting for approximately 71% of this explanatory power (i.e., approximately 35% of the total variability in size distributions). Note that the correlation captures concurrent shifts in the distribution of environmental conditions and euphausiid size structure, and does

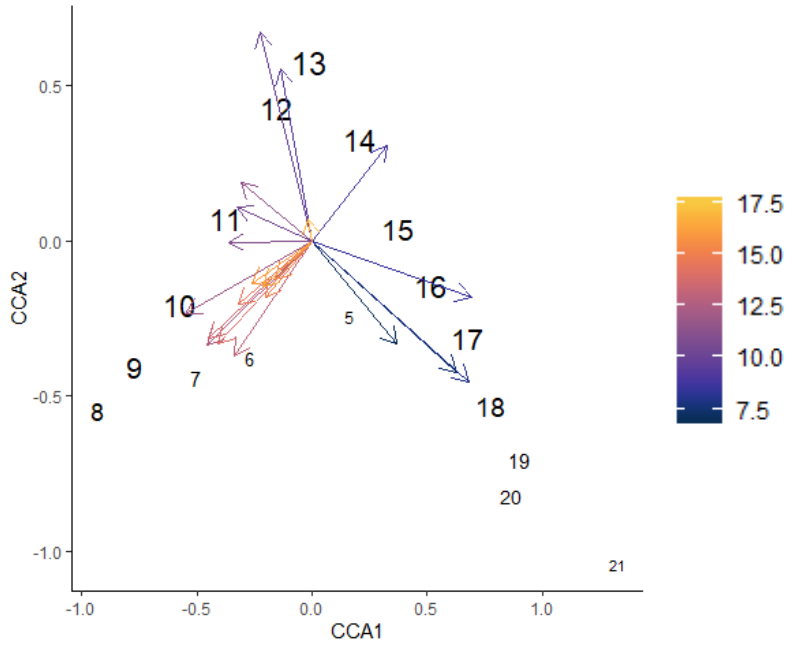

Fig. 9. Canonical correspondence analysis of adult *Euphausia pacifica* mean body length distributions (mm; indicated by number on plot) and the distribution of temperature (m of water column included in 0.5°C bins) aggregated over all stations ($p < 0.01$). Numbers indicate mid-point of adult size class and scale approximately with relative representation of that size class in the entire data set. Vector color indicates midpoint of temperature bins. The first two axes (CCA1 and CCA2; eigenvectors) account for approximately 71% of the variability explained by the CCA and approximately 35% of the total variability in the data.

not imply explicit co-location of euphausiids of a particular size with water of a particular temperature.

3.6 Abundance

Abundance of adult *E. pacifica* varies by over an order of magnitude over the course of the time series. Adults are, in general, present year-round and a clear seasonal trend in abundance is not apparent.

Adults were absent from our collections on only rare occasions, most notably during a single cruise in early 2016 that was strongly influenced by poleward transport associated with the 2015-16 El Niño.

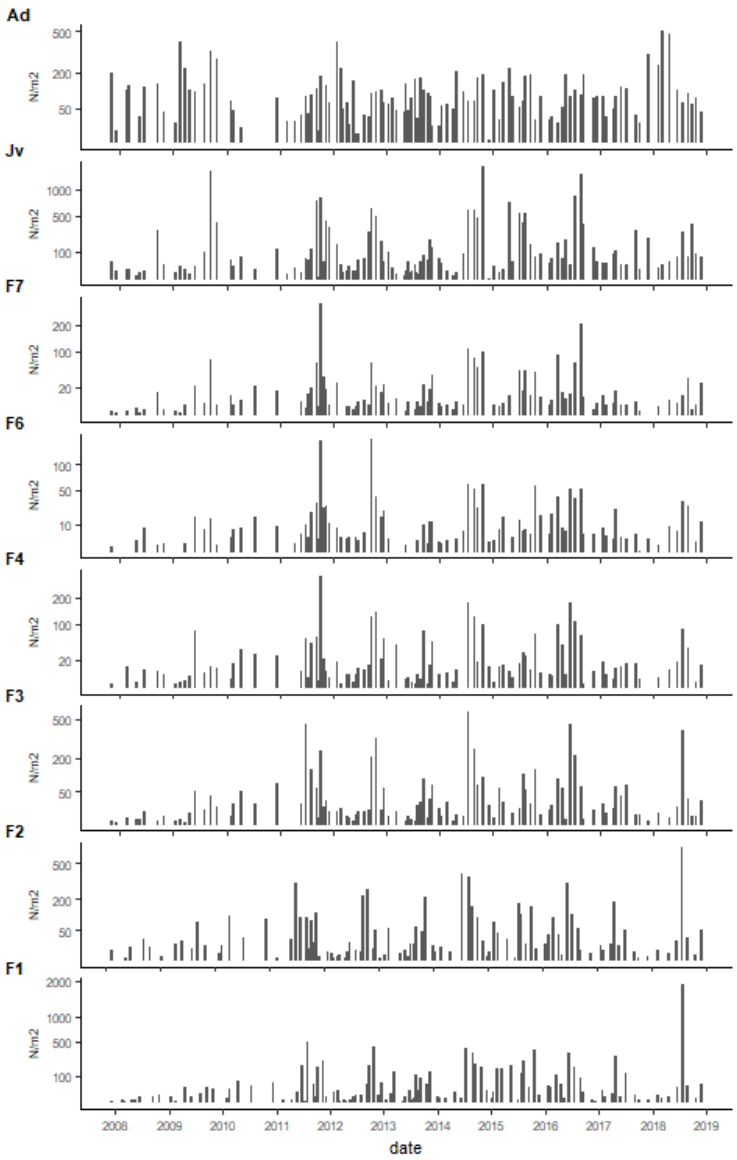

Fig. 10. Stage-specific mean areal density (N m^{-2}; y-axis)) of *Euphausia pacifica* across all stations by cruise date (x-axis). From top to bottom: adults (Ad), juveniles (Jv) and furcilia stages F7-F1. Note that the y-axis indicates areal density on a square-root-transformed scale.

In contrast, immature life history stages exhibited much greater variability in abundance over time, (Fig. 10). All stages were encountered throughout the year across the time series, with strong seasonal maxima in abundance typically observed during spring and summer. Abundance of furcilia, at least

during peak seasons, appears to have increased following the 2009-10 El Niño and to have declined again during the 2015-16 El Niño. Following relatively high densities in summer 2016, furcilia abundance was again relatively low throughout 2017. Except for a single cruise during summer, when densities of F1-F3 furcilia were exceptionally high, furcilia abundance during 2018 remained relatively low.

3.7 Variability in individual and population biomass

The biomass (in µg C) of an adult *E. pacifica* of average size (2527 µg C) greatly exceeds that of an average juvenile (332 µg C), intermediate furcilia (e.g., F4/5; 44 µg C), or early furcilia (F1; 8 µg C) (Table 1). Within the range of adult size, individual biomass can vary by a factor of 40 or more (e.g., approximately 225 µg C at 6 mm to approximately 8700 µg C at 19 mm). Accordingly, variability in biomass of *E. pacifica* along the Trinidad Head Line is dominated by changes in adult abundance and (especially) size (Fig. 11).

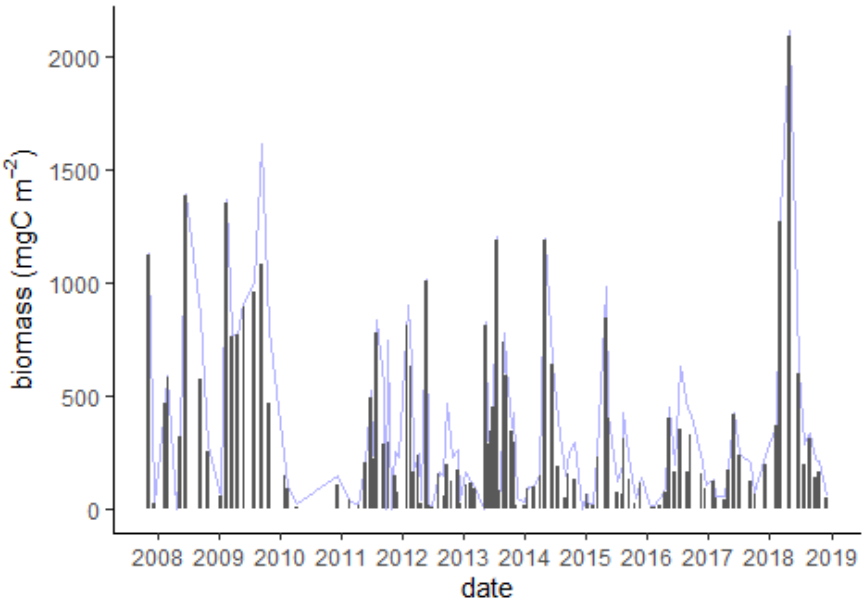

Fig. 11. Mean biomass (by areal density) of adult (black bars) and F1 furcilia-adult stages of *Euphausia pacifica* (blue line) aggregated across stations along the Trinidad Head Line.

Biomass of adult *E. pacifica* tends to be relatively low during fall and winter months and high during spring and early summer months, and responds sharply to rapid transitions in population size structure, such as the sharp drop in biomass concurrent with the similarly dramatic decline in mean adult size during the arrival of warm blob in late 2014. Except for a seasonal pulse related to strong upwelling in

2015, biomass remained relatively low throughout the 2014-16 MHW. A brief increase in biomass during spring 2018 reflects unusually high abundance of adult *E. pacifica* (Fig. 10) coupled with an increase in adult size following the MHW (Fig. 6).

4. Discussion

Through the development and analysis of detailed information on length, life-history stage, and abundance, we document the strong effect of warm climate events on the size distributions of *Euphausia pacifica* in coastal waters off northern California. This pattern was especially apparent during the 2014 – 16 MHW, when we captured numerous mature individuals smaller than any previously reported in the literature and larger size classes were conspicuously absent or rare. Further, by including in our analysis assessment of earlier life history stages, we find that furcilia exhibit a contrasting response to climatic variability, in which larger size classes of furcilia are associated with warmer conditions.

Our analysis reveals that climate variability modulates seasonal trends in size distributions of *E. pacifica* in coastal waters off northern California, and indicates that changes in both temperature and chlorophyll concentration (or some unmeasured factor correlated with these parameters) drive these dynamics. *We* focus on the hypothesis that variability in temperature is the main driver of shifts in size distributions across years. This is in part, a *recognition that temperature is a powerful proxy for ocean dynamics that influence ecosystem state*, as well as a reflection of clear patterns in the data: temperature varies dramatically across years, especially during non-upwelling seasons, whereas chlorophyll concentration does not exhibit a consistent response to climate forcing (Fig. 5). Including chlorophyll concentration as a covariate in models relating size to environmental conditions reflects the common observation that, all else constant, more food typically supports greater growth. In contrast, allowing the response to temperature to include random year-to-year (i.e., climate) effects is consistent with the role of temperature in controlling organisms' metabolism, thereby determining the rate at which individuals can grow when food is not limiting, and more generally, the amount of surplus energy available from a given amount of food. Surplus energy, whether as an instantaneous measure or as a predictor of future resources, is a powerful driver of life history decisions regarding size-at-maturation and the allocation of energy towards growth or reproduction (Mangel and Ludwig, 1992, Siegel, 2000; Poleck and Denys, 1982; Jager and Ravagnan, 2015; Constable and Kawaguchi, 2018). This effect of

559 temperature on population structure appears to be fundamental to the patterns we observed in our
560 data.
561
562 Before proceeding, we note that various sources of potential sampling bias (e.g., net avoidance, vertical
563 migration) appear to have little substantive effect on our data and analysis. While mid- and inner-shelf
564 stations are sampled during daylight hours when net avoidance by larger euphausiids is more likely than
565 during night-sampling, adult *E. pacifica* are seldom found during either day or night in shelf waters (L.
566 Feinberg *personal communication* in Gómez-Gutiérrez et al., 2005; Bjorkstedt and Robertson, in prep.;
567 unpublished data from THL cruises when all stations were occupied during darkness). Moreover, shelf
568 samples containing adult *E. pacifica* and *T. spinifera* indicate our gear is capable of capturing adult
569 euphausiids during daylight hours when they are present in waters over the shelf (Bjorkstedt and
570 Robertson, in prep.). Because sampling at TH03 occurs just prior to darkness and the entire water
571 column is not sampled, underestimation of adult abundance may occur. However, consistent size
572 distributions between TH03 and offshore stations suggest samples from TH03 accurately represent
573 population size structure (Fig. 4).
574
575 **4.1 Seasonal, Interannual, and Ontogenetic Patterns**
576 Size distributions of adult *E. pacifica* reached seasonal maxima during spring and summer, coincident
577 with periods of higher productivity and conditions supportive of growth (Smiles and Pearcy, 1971;
578 Tanasichuk, 1998). Climate variability modulates this seasonal pattern, as demonstrated by sharp
579 declines in the size of adult *E. pacifica* – declines on the order of 30-40% of average size concurrent with
580 the arrival in late 2014 of unusually warm waters associated with the 'warm blob' (Bond et al., 2015).
581 The shift towards small size distributions of adult *E. pacifica* persisted into and through continued warm
582 conditions associated with the 2015-16 El Niño (Chao et al., 2017). Similar dynamics were reported from
583 collections along the Newport Hydrographic Line off Oregon (44.2°N), where in 2015 the average length
584 of adult *E. pacifica* was several millimeters smaller than any previous observations (Peterson et al.,
585 2017). Climate variability also drives more subtle variability in size distributions among years which
586 manifests as smaller sizes during years with delayed onset of upwelling (e.g., 2012; Wells et al., 2013) or
587 recovery from moderate El Niño conditions (e.g., 2010) and larger size during years marked by intense
588 upwelling (e.g., 2008, 2013). In general, these patterns are consistent with negative correlations
589 between individual adult *E. pacifica* weight and SST (Abraham and Sydeman, 2006), and similar, though

590 less clearly resolved responses in adult *Thysanoessa spinifera* and *Nematoscelis difficilis* from our
591 collections off northern California (unpublished data).
592
593 Our analysis revealed ontogenetic trends in correlation between *E. pacifica* body size and temperature:
594 adults and juveniles exhibited a clear shift to smaller size distributions under warmer conditions while
595 the opposite pattern was observed for furcilia. These patterns are consistent with stage-dependent
596 temperature-size relationships reported for diverse marine taxa, including crustaceans (Forster and
597 Hirst, 2012). These observations, in conjunction with the ability of adult *E. pacifica* to shrink in response
598 to food limitation or elevated temperature (Pinchuk and Hopcroft, 2007; Marinovic and Mangel, 1999)
599 suggest that *E. pacifica* has a highly plastic life history, in which the timing and size of stage transitions—
600 including, especially, maturation—are governed by a temperature-dependent balance between energy
601 intake and metabolism (Angilletta and Angilletta, 2009) in the context of size-dependent predation
602 (Peterson and Wroblewski, 1984) and reproductive output (Gómez-Gutiérrez et al., 2006).
603
604 The magnitude of change in biomass in response to temperature estimated in this study (-24% $°C^{-1}$ for
605 adults) exceeds estimates of similar responses in marine crustaceans (maximum decline of 8%; ~2% for
606 *E. pacifica*; Forster et al., 2012). We suspect that part of this discrepancy is due to our use of average
607 water temperature over the entire water column (1:100 m max) rather than temperature specific to
608 where individuals reside. Consequently, estimates of percent change in relation to temperature
609 reported here should be treated with caution when compared to laboratory experiments.
610
611 **4.2 Mechanisms**
612 Several non-exclusive mechanisms offer plausible explanations for observed shifts in the size structure
613 of euphausiid populations in the upper water column off northern California, and may be broadly
614 categorized as those dominated by movement of water masses (i.e., advection or displacement) and
615 those arising from ecological interactions and physiological processes (Dorman et al., 2011). Here we
616 describe and evaluate these hypotheses, keeping in mind that the data available to us represent
617 snapshots of growth processes that integrate organisms' exposure to multiple factors (i.e., temperature
618 and food) over time in a highly dynamic environment.
619
620 Horizontal advection of warm water masses into the sampling region is, we believe, the dominant cause
621 of rapid shifts in size distributions of adult *E. pacifica* and in particular the presence of small individuals.

622 The underlying assumption that dissimilar water masses host populations with distinct size distributions
623 is consistent with generally strong biogeographic associations between water mass characteristics and
624 zooplankton assemblages or indicator species (Hooff and Peterson, 2006; Kiester et al., 2005). This
625 hypothesis draws further support from physical modeling studies (e.g., Chao et al., 2017) that indicate
626 anomalous onshore transport of warm water during the arrival of the warm 'blob' in 2014 and poleward
627 transport of warm water during the 2015-16 El Niño. Concurrent shifts in copepod assemblages, and the
628 sequential arrival of *Euphausia recurva* (in early 2015) and *Nyctiphanes simplex* (in late 2015), indicators
629 of onshore and poleward transport, respectively, in the northern CCE (Keister et al., 2005), further
630 corroborate the influence of anomalous transport on coastal waters (McClatchie et al., 2016; Wells et
631 al., 2017; Bjorkstedt and Robertson, in prep.). Warm water anomalies also brought a highly unusual
632 pelagic assemblage dominated by pyrosomes and other gelatinous taxa into coastal waters (Sakuma et
633 al., 2016).
634
635 We suspect that the disappearance of larger individuals from our samples is also, at least in part, driven
636 by vertical displacement associated with the arrival of warm water masses and depression of the
637 thermocline. If large adults are closely associated with cooler water, such displacements could push
638 large adults beyond the reach of our net tows. It is difficult to assess this possibility without additional,
639 deeper sampling, or possibly comparison to coincident acoustic observations. However, large adults
640 rapidly disappeared from our collections in late 2014, but made an equally rapid return and
641 disappearance during a brief window of strong upwelling in early 2015, suggesting that these individuals
642 had not been displaced substantial distances, nor had they suffered acute mortality.
643
644 Robust correlation in mean size across larval stages (Table 2) is also consistent with
645 advection/displacement hypotheses in that it suggests that individuals spanning several life history
646 stages have experienced similar conditions for periods extending from days to weeks, but is also likely to
647 reflect coherence in production and growth at seasonal scales (Fig. 5). Correlations tend to be strongest
648 between sequential larval stages, where time between stages is on the order of days (Ross, 1981;
649 Feinberg et al., 2006) and similar environmental exposure histories may be expected to yield parallel
650 growth patterns. The correlation between F1 furcilia and adults and breakdown of correlations between
651 adults and more advanced furcilia stages might reflect, at least in part, a divergence in environmental
652 conditions experienced over time, and is consistent with observations of declining spatial overlap
653 between adult and larval stage *E. pacifica* elsewhere in the California Current (Décima et al., 2010).

654
655 It is less clear that shrinking in response to warming temperatures or reduction in food availability
656 (Marinovic and Mangel, 1999; Pinchuk and Hopcroft, 2007; Shaw et al. 2010) or ecological interactions
657 such as changes in size-dependent mortality (starvation or predation), might substantively account for
658 our observations, particularly in the case of rapid shifts in size structure. On several occasions, however,
659 rates of decline in mean size of euphausiids in our samples exceeded rates of shrinking reported for
660 individual *E. pacifica* (Shaw et al., 2010; Marinovic and Mangel 1999; Pinchuk and Hopcroft, 2007). We
661 have no data with which to rigorously assess short-term variability in predation. Our record does not
662 span conditions similar to those observed in 2005, in which persistent suppression of upwelling
663 throughout much of the spring and early summer is hypothesized to have driven extensive starvation
664 mortality of krill in the CCE (Dorman et al., 2011).
665
666 Although rapid growth- or predation-dependent mechanisms seem less plausible as a cause of rapid
667 shifts in size-structure of *E. pacifica*, ecological and physiological processes must underpin persistent
668 differences in size-structure related to water mass characteristics, and thus establish conditions
669 necessary for transport processes to drive temporal variability at local scales as discussed above. At
670 present, we are unable to resolve whether the small juvenile and adult *E. pacifica* observed in our
671 samples had previously achieved a larger size and then shrank or had developed along a fixed
672 temperature-dependent trajectory (but see Shin et al., 2002). Such information would support a more
673 definitive assessment of underlying mechanisms. The capacity for krill to shrink during bouts of intense
674 reproduction suggests the potential for even more rapid changes in body mass than might be expected
675 through somatic metabolism (Feinberg et al., 2007).
676
677 Our analysis identified a relationship between chlorophyll concentration and euphausiid size that is
678 consistent with the hypothesis that euphausiid growth in the CCE is driven by upwelling-fueled primary
679 production (Shaw et al., 2010), and might partly explain more subtle changes in size structure from year
680 to year (e.g., in response to the delayed onset of upwelling in 2012; Wells et al. 2013). However, high
681 chlorophyll concentrations during the warm anomaly were commonly associated with persistent,
682 recurring blooms of *Pseudo-nitzschia spp*. that generated high concentrations of domoic acid along the
683 THL during summer months from 2014 through 2016 (unpublished data), reaching record levels during
684 an extensive and persistent harmful algal bloom in 2015 (McCabe et al., 2016). Sustained exposure to
685 domoic acid have been shown to suppress feeding in euphausiids (Bargu et al., 2006), with obvious

consequences for growth rates. The potential for an interaction between elevated temperatures and changes in food quality in driving the decline in adult size during the 2014-16 MHW cannot be ruled out, leaving open the possibility that variability in size reflects a stronger and more variable influence of trophic mechanisms at longer (interannual) time scales.

4.3 Ecological Implications

Regardless of specific mechanisms and drivers, changes in the size structure of critical forage species like *E. pacifica* have the potential to trigger ecological responses in coastal waters of the CCE. Sustained reduction in average size and biomass of *E. pacifica*, such as we observed during the 2014-16 MHW, almost certainly reduced the availability of *E. pacifica* as forage for diverse predator species ranging from generalists such as salmon or rockfishes to those that more specifically target euphausiids as prey (e.g., some baleen whales and seabirds). Moreover, the general shift towards smaller size across the population means that what biomass is available to predators comes in smaller packages, which influences how efficiently predators, especially those that target individual prey, accumulate energy (e.g., Lovvorn, 2010). Consequences for higher trophic levels can be profound. For example, a sustained shift in the structure and distribution of euphausiid populations is suspected to have played a role in a massive mortality event affecting Cassin's auklet (*Ptychoramphus aleuticus*) from northern California to Alaska during the 2014-16 MHW (Jones et al., 2018). Moreover, seasonal trajectories of E. pacifica size distributions appear to have been set early in the year, so that the size of adult E. pacifica during the height of the upwelling season depends strongly on conditions during the preceding winter, whether through persistent changes in ecosystem productivity and environmental conditions, as a consequence of intrinsic demographic or physiological inertia, or arising from some other mechanism(s). From the perspective of understanding impacts on higher trophic levels, our findings enrich support for "preconditioning" hypotheses that emphasize the importance of environmental conditions in late winter—prior to the onset of sustained seasonal upwelling—as a key determinant of productivity in the California Current (Logerwell et al., 2003; Black et al., 2010; Schroeder et al., 2013).

Variability in the size structure of *E. pacifica* (and other euphausiids) also has the potential to impact species upon which euphausiids prey, including copepods (Ohman, 1986; Stuart and Pillar, 1990) and eggs and larvae of marine fishes (Bailey, et al. 1993, Theilacker, et al. 1993). Based on evidence that the susceptibility of larval fish to predation depends on the size of the predator relative to its prey (Paradis

et al. 1996), changes in the average size of adult *E. pacifica* off northern California might contribute to substantial variation in predation pressure on larval fishes in coastal waters.

4.4 Connecting data to models

Rigorous assessment of mechanisms that link population dynamics to environmental conditions will require models that integrate the concurrent effects of multiple factors (i.e., temperature and food) on the growth and development of *E. pacifica*. Coupling individual-based models and life history theory to realistic models of ocean circulation and productivity offer a way to examine this dynamic under different conditions and to parse out the contributions of advection versus production (Dorman et al., 2015b). In more complex frameworks, modeling exposure to currents and predators will require accounting for size-dependence in vertical distributions and migration (Duarte, 2007; O'Connor et al., 2007). The validity and utility of such approaches, however, will depend on accurately representing plasticity in the growth and maturation responses of *E. pacifica* to environmental conditions. Successful development and evaluation of such models depends on high-quality empirical data, whether derived from laboratory experiments (e.g., Ross 1979; Feinberg et al., 2006) or from careful analysis of samples collected in the field to complement existing observations on spatial distributions (Gómez-Gutiérrez et al., 2005; Lamb and Peterson, 2005; Lindsey and Batchelder, 2011)

This study clearly illustrates the potential return on such effort. Our data set is one of few that provide detailed information on size distributions across a broad range of developmental stages of *E. pacifica* (Boden, 1950; Brinton and Wyllie, 1976; Ross 1979). Moreover, detailed morphological analysis revealed shifts in stage-specific size distributions of adults and juveniles that would have been misinterpreted as changes in abundance for each life history stage had stage-designations been based solely on size thresholds. Over the course of the time series, about 3% of adult *E. pacifica* were below minimum size thresholds reported in the literature and often applied to delineate adults from juveniles in analysis of plankton samples (e.g., 10-11 mm TL or about 8 mm BL; Brinton, 1976; Brinton and Wyllie, 1976; Bollens, 1992; Ju et al., 2009). Conversely, about 26% of juveniles exceeded size thresholds and would have been designated as adults. These proportions vary as size distributions shift over time. For example, for 2013, 1% of adults and 34% of juveniles would have been misclassified, whereas 11% and 12% of adults and juveniles, respectively, would have been misclassified during the 2014-16 MHW. Actual discrepancies in population structure will depend on the (true) ratio of adults and juveniles in the population. Errors in stage designation will not affect estimates of biomass that do not discriminate

among stages or that are based on individuals that satisfy length criteria. Morphological stage-designations, however, appear to be essential if data are to provide unbiased information to support demographic models for euphausiid population dynamics or studies focused on understanding how life history strategies and evolution are affected by environmental and climate variability.

5. Conclusion

Warm water events are expected to increase in frequency and duration with ongoing climate change (Frölicher et al., 2018; Oliver et al., 2018). We show that such an event can drive strong shifts in size-distributions of a dominant euphausiid species in coastal waters off northern California. Moreover, our data confirm that warming events can disrupt or suppress typical seasonal patterns (i.e., the tendency for mean size of adult euphausiids to increase through the spring and summer upwelling season), leading to persistent transitions towards adult and juvenile length distributions dominated by smaller size classes. Given the central role of *E. pacifica* in trophic dynamics of the CCE, and the sensitivity of several higher trophic levels to the timing and magnitude of prey production (Abraham and Sydeman, 2004; Wolf et al., 2010, Wells et al., 2012), such dynamics have profound implications for ecosystem-level responses to warming events and climate change in general. Accordingly, time series of adult *E. pacifica* size have been incorporated into NOAA's California Current Integrated Ecosystem Assessment as an indicator for lower trophic level productivity and ocean-ecosystem health (Harvey et al., 2019). More generally, our results complement other work (Peterson et al., 2017; McCabe et al., 2016; Jones et al., 2018; Cavole et al., 2016) in fulfilling the need for information on a multitude of processes, ranging from individual to ecosystem, to understand marine ecosystem responses to climate and environmental variability (Beaugrand and Kirby, 2018).

These insights would not be possible without detailed analysis of plankton samples, which highlights the unique capability of long-term net sampling to reveal important biological signals not yet resolved by other zooplankton sampling methods. Data from careful taxonomic and morphological analysis of in-hand samples contain information essential for corroborating and enriching more extensive sampling methods (e.g., acoustics and optics) in terms of community composition, demographic and size structure, and for advancing the development of population and ecosystem models. For this reason, high frequency, long-term sampling as part of a comprehensive observing program presently remains

780 essential for resolving the response of euphausiids and the broader zooplankton community to climate
781 variability and understanding their roles in dynamic ecosystems (Bjorkstedt and Peterson, 2015).
782
783 **Acknowledgements**
784 Sampling along the Trinidad Head Line has been supported by NOAA's Southwest Fisheries Science
785 Center both directly and through the Cooperative Institute for Marine Ecosystems and Climate, in
786 collaboration with Humboldt State University. We thank Phil White, Abby Johnson, Kathryn Crane, and
787 Ashok Sadrosinski for serving as lead scientists during THL cruises, and Caymin Ackerman, Winn
788 McEnery, Erin Damm, and Spencer Hitzeroth for their contributions to the euphausiid dataset. We also
789 thank the Captain and crew of the *R/V* Coral Sea and all of the student volunteers and assistants for
790 their able support of the THL sampling program. Keith Sakuma, John Field, Angus Atkinson, and an
791 anonymous reviewer for providing insightful reviews that improved the manuscript. Lastly, we thank Bill
792 Peterson for his mentorship and enthusiastic support in making the Trinidad Head Line a reality; his was
793 a valued friendship and collaboration cut far too short and deeply missed.
794
795 **Appendix A. Supplemental Material**
796
797 **References**
798
799 Abraham, C., W. Sydeman (2004), Ocean climate, euphausiids and auklet nesting: inter-annual trends
800 and variation in phenology, diet and growth of a planktivorous seabird, *Ptychoramphus*
801 *aleuticus*, *Mar. Ecol. Prog. Ser.,* 274, 235-250, https://doi.org/10.3354/meps274235.
802 Abraham, C., W. Sydeman (2006), Prey-switching by Cassin's auklet *Ptychoramphus aleuticus* reveals
803 seasonal climate-related cycles of *Euphausia pacifica* and *Thysanoessa spinifera*, *Mar. Ecol. Prog.*
804 *Ser.*, *313*, 271-283, https://doi.org/10.3354/meps313271.
805 Angilletta Jr, M. J., M. J. Angilletta (2009), *Thermal adaptation: a theoretical and empirical synthesis*,
806 Oxford University Press.
807 Atkinson, D. (1994), Temperature and organism size: A biological law for ectotherms? *Adv. Ecol. Res.*, 25,
808 1-58.
809 Bailey, K. M., R. D. Brodeur, N. Merati, A.M.M. Yoklavich (1993), Predation on walleye pollock (*Theragra*
810 *chakograrnma*) eggs and yolk-sac larvae by pelagic crustacean invertebrates in the western Gulf
811 of Alaska, *Fish. Oceanogr.*, 2(1), 30-39.

812 Bargu, S., K. Lefebvre, M. W. Silver (2006), Effect of dissolved domoic acid on the grazing rate of krill
813 *Euphausia pacifica*, *Mar. Ecol. Prog. Ser.,* 312, 169-175, http://doi.org/10.3354/meps312169.
814 Barth, J. A., S. D. Pierce, R. L. Smith (2000), A separating coastal upwelling jet at Cape Blanco, Oregon
815 and its connection to the California Current System, *Deep-Sea Res. Pt. II,* 47, 783-810,
816 https://doi.org/10.1016/S0967-0645(99)00127-7.
817 Bartoń, K. (2019), MuMIn: Multi-Model Inference. R package version 1.43.6., https://CRAN.R-
818 project.org/package=MuMIn.
819 Batteen, M. (1997), Wind-forced modeling studies of currents, meanders, and eddies in the California
820 Current system, *J. Geophys. Res*., 102, 985-1010, https://doi.org/10.1029/96JC02803.
821 Beaugrand, G., R. R. Kirby (2018), How do marine pelagic species respond to climate change? Theories
822 and observations, *Annu. Rev. Mar. Sci.*, *10*, 169-197, https://doi.org/10.1146/annurev-marine-
823 121916-063304.
824 Becker, B. H., M. Z. Peery, S. R. Beissinger (2007), Ocean climate and prey availability affect the trophic
825 level and reproductive success of the marbled murrelet, an endangered seabird, *Mar. Ecol. Prog.*
826 *Ser.*, 329, 267-279, https://doi.org/10.3354/meps329267.
827 Bjorkstedt E., W. Peterson (2015), Zooplankton data from high-frequency coastal transects: enriching
828 the contributions of ocean observing systems to ecosystem-based management in the northern
829 California Current, Pages 199-142 in Y. Liu, H. Kerkering, and R.H. Weisberg (eds). Coastal Ocean
830 Observing Systems: Advances and Syntheses. Elselvier.
831 Black, B. A., I. D. Schroeder, W. J. Sydeman, S. J. Bograd, P. W. Lawson (2010), Wintertime ocean
832 conditions synchronize rockfish growth and seabird reproduction in the central California
833 Current ecosystem, *Can. J. Fish. Aquat. Sci.*, *67*(7), 1149-1158.
834 Boden, B. P. (1950), The post-naupliar stages of the crustacean *Euphausia pacifica*, *Trans. Am. Microsc.*
835 *Soc.*, *69*(4), 373-386.
836 Bollens, S. M., B.W. Frost, T. S. Lin (1992), Recruitment, growth, and diel vertical migration of *Euphausia*
837 *pacifica* in a temperate fjord, *Mar. Bio.*, *114*(2),219-228, https://doi.org/10.1007/BF00349522.
838 Bond, N., M. F. Cronin, H. Freeland, N. Mantua (2015), Causes and impacts of the 2014 warm anomaly in
839 the NE Pacific, *Geophys. Res. Lett.,* 42(9) 3414-3420, https://doi.org/10.1002/2015GL063306.
840 Brinton, E. (1965), Vertical migration and avoidance capability of euphausiids in the California Current,
841 *Limnol. Oceanogr.,* 12(3), 451-483, https://doi.org/10.4319/lo.1967.12.3.0451.
842 Brinton, E. (1976), Population biology of *Euphausia pacifica* off southern California, *Fish. Bull.,* 74(4),
843 733-762.

844 Brinton, E., J. G. Wyllie (1976), Distributional atlas of euphausiid growth stages off southern California,
845 1953 through 1956 (No. 24). Marine Life Research Program, Scripps Institution of Oceanography.
846 Brinton, E., M. D. Ohman, A. W. Townsend, M.D. Knight, A. L. Bridgeman (1999), Euphausiids of the
847 world ocean, World Biodiversity Database CD-ROM Series, Springer Verlag Electronic Media.
848 Brinton, E., A. Townsend (2003), Decadal variability in abundances of the dominant euphausiid species in
849 southern sectors of the California Current, *Deep-Sea Res. Pt. II,* 50, 2449-2472,
850 https://doi.org/10.1016/S0967-0645(03)00126-7.
851 Brodeur, R. D., W. G. Pearcy (1992), Effects of environmental variability on trophic interactions and food
852 web structure in a pelagic upwelling ecosystem, *Mar. Ecol. Prog. Ser.,* 84, 101-119,
853 https://doi.org/10.3354/meps084101.
854 Cavole, L. M., A. M. Demko, R. E. Diner, A. Giddings, I. Koester, C. M. Pagniello, M. L. Paulsen, A.
855 Ramirez-Valdez, S. M. Schwenck, N. K. Yen, M. E. Zill (2016), Biological impacts of the 2013-2015
856 warm-water anomaly in the Northeast Pacific: Winners, losers, and the future, *Oceanography,*
857 29(2), 273-85, https://doi.org/10.5670/oceanog.2016.32.
858 Chao, Y., J. D. Farrara,E. Bjorkstedt, F. Chai, F. Chavez, D. L. Rudnick, W. Enright, J. L. Fisher, W. T.
859 Peterson, G. F. Welch, C. O. Davis (2017), The origins of the anomalous warming in the California
860 coastal ocean and San Francisco Bay during 2014–2016, *J. Geophys. Res*. *Oceans*, *122*(9), 7537-
861 7557, https://doi.org/10.1002/2017JC013120.
862 Constable, A. J., S. Kawaguchi (2018), Modelling growth and reproduction of Antarctic krill, *Euphausia*
863 *superba*, based on temperature, food and resource allocation amongst life history functions,
864 *ICES J. Mar. Sci.,* 75(2), 738-750.
865 Daufresne, M., K. Lengfellner, U. Sommer (2009), Global warming benefits the small in aquatic
866 ecosystems, *PNAS*, 106,12788-12793, https://doi.org/10.1073/pnas.0902080106.
867 Décima, M. M. D. Ohman, A. D. Robertis (2010), Body size dependence of euphausiid spatial patchiness,
868 *Limnol. Oceanogr.* 55(2) 777-788, https://doi.org/10.4319/lo.2010.55.2.0777.
869 Dilling, L., J. Wilson, D. Steinberg, A. Alldredge (1998), Feeding by the euphausiid *Euphausia pacifica* and
870 the copepod *Calanus pacificus* on marine snow, *Mar. Ecol. Prog. Ser.*, 170, 189-201.
871 Dorman, J. G., S. M. Bollens, A. M. Slaughter (2005), Population biology of euphausiids off northern
872 California and effects of short time-scale wind events on *Euphausia pacifica*, *Mar. Ecol. Prog.*
873 *Ser*., *288*, 183-198.

874 Dorman, J. G., T. M. Powell, W. J. Sydeman, S. J. Bograd (2011), Advection and starvation cause krill
875 (*Euphausia pacifica*) decreases in 2005 Northern California coastal populations: Implications
876 from a model study, *Geophys. Res. Lett*., 38(4).
877 Dorman, J. G., W. J. Sydeman, M. Garcia-Reyes, R. A. Zeno, J. A. Santora (2015a), Modeling krill
878 aggregations in the central-northern California Current, *Mar. Ecol. Prog. Ser.,* 528, 87-99,
879 https://doi.org/10.3354/meps11253.
880 Dorman, J. G., W. J. Sydeman, S. J. Bograd, T. M. Powell (2015b), An individual-based model of the krill
881 Euphausia pacifica in the California Current, *Prog. Oceangr*., 138, 504-520,
882 http://dx.doi.org/10.1016/j.pocean.2015.02.006.
883 Du, X., W. Peterson (2014), Feeding rates and selectivity of adult *Euphausia pacifica* on natural particle
884 assemblages in the coastal upwelling zone off Oregon, USA, 2010, *J. Plankton Res*., 36(4), 1031-
885 1046.
886 Duarte, C.M. (2007), Marine ecology warms up to theory, *Trends Ecol. Evol.* 22(7), 331-333,
887 https://doi.org/10.1016/j.tree.2007.04.001.
888 Fiechter, J., J. A. Santora, F. Chavez, D. Northcott, M. Messié (2020), Krill hotspot formation and
889 phenology in the California Current Ecosystem, *Geophys. Res. Lett.*, 47, p.e2020GL088039,
890 https://doi.org/10.1029/2020GL088039.
891 Feinberg, L. R., C. T. Shaw, W. T. Peterson (2006), Larval development of *Euphausia pacifica* in the
892 laboratory: variability in developmental pathways, *Mar. Ecol. Prog. Ser.*, *316*, 127-137,
893 https://doi.org/10.3354/meps316127.
894 Feinberg, L. R., C. T. Shaw, W. T. Peterson (2007), Long-term laboratory observations of *Euphausia*
895 *pacifica* fecundity: comparison of two geographic regions, *Mar. Ecol. Prog. Ser.*, *341*, 141-152,
896 https://doi.org/10.3354/meps341141.
897 Field, J. C., R. C. Francis, K. Aydin (2006), Top-down modeling and bottom-up dynamics: Linking a
898 fisheries-based ecosystem model with climate hypotheses in the Northern California Current,
899 *Prog. Oceanogr.,* 68, 238-270, https://doi.org/10.1016/j.pocean.2006.02.010.
900 Forster, J., A. G. Hirst (2012), The temperature-size rule emerges from ontogenetic differences between
901 growth and development rates, *Funct. Ecol.*, *26*(2), 483-492, https://doi.org/10.1111/j.1365-
902 2435.2011.01958.x.
903 Forster, J., A. G. Hirst, D. Atkinson (2012), Warming-induced reductions in body size are greater in
904 aquatic than terrestrial species, *PNAS*, *109*(47), 19310-19314,
905 https://doi.org/10.1073/pnas.1210460109.

906 Fowler, S.W., L. F. Small, S. Kečkeš (1971), Effects of temperature and size on molting of euphausiid
907 crustaceans, *Mar. Bio.*, *11*(1), 45-51, https://doi.org/10.1007/BF00348020.
908 Frölicher, T. L., E. M. Fischer, N., Gruber (2018), Marine heatwaves under global
909 warming, *Nature*, *560*(7718), 360, https://doi.org/10.1038/s41586-018-0383-9.
910 Garcia-Reyes, M., J. Largier (2012), Seasonality of coastal upwelling off central and northern California, *J.*
911 *Geophys. Res. Oceans,* 117(C3), https://dx.doi.org/10.1029/2011JC007629.
912 Gentemann, C. L., M. R. Fewings, M. Garcia-Reyes (2016), Satellite sea surface temperatures along the
913 West Coast of the United States during the 2014-2016 northeast Pacific marine heat wave,
914 *Geophys. Res. Lett.,* 44, 312-319, https://doi.org/10.1002/2016GL071039.
915 Gómez-Gutiérrez, J., W. T. Peterson, C. B. Miller (2005), Cross-shelf life-stage segregation and
916 community structure of the euphausiids off central Oregon, *Deep Sea Res. Pt. II,* 52(1), 289-315,
917 https://doi.org/10.1016/j.dsr2.2004.09.023.
918 Gómez-Gutiérrez, J., L. R. Feinberg, T. Shaw, W. T. Peterson (2006), Variability in brood size and female
919 length of *Euphausia pacifica* among three populations in the North Pacific, *Mar. Ecol. Prog. Ser.*,
920 323, 185-194, https://doi.org/10.3354/meps323185.
921 González, H. E., M. Sobarzo, M., D. Figueroa, E. M Nöthig (2000), Composition, biomass and potential
922 grazing impact of the crustacean and pelagic tunicates in the northern Humboldt Current area
923 off Chile: differences between El Niño and non-El Niño years, *Mar. Ecol. Prog. Ser., 195*, 201-220.
924 Harvey, C., N. Garfield, G. Williams, N. Tolimieri, I. Schroeder, K. Andrews, K. Barnas, E. Bjorkstedt, S.
925 Bograd, R. Brodeur, B. Burke, J. Cope, A. Coyne, L. deWitt, J. Dowell, J. Field, J. Fisher, P. Frey, T.
926 Good, C. Greene, E. Hazen, D. Holland, M. Hunter, K. Jacobson, M. Jacox, C. Juhasz, I. Kaplan, S.
927 Kasperski, D. Lawson, A. Leising, A. Manderson, S. Melin, S. Moore, C. Morgan, B. Muhling, S.
928 Munsch, K. Norman, R. Robertson, L. Rogers-Bennett, K. Sakuma, J. Samhouri, R. Selden, S.
929 Siedlecki, K. Somers, W. Sydeman, A. Thompson, J. Thorson, D. Tommasi, V. Trainer, A. Varney,
930 B. Wells, C. Whitmire, M. Williams, T. Williams, J. Zamon, S. Zeman (2019), Ecosystem Status
931 Report of the California Current for 2019: A Summary of Ecosystem Indicators Compiled by the
932 California Current Integrated Ecosystem Assessment Team (CCEIA), U.S. Department of
933 Commerce, NOAA Technical Memorandum NMFS-NWFSC-149, https://doi.org/10.25923/p0ed-
934 ke21.
935 Hasselblad, V. (1966), Estimation of parameters for a mixture of normal distributions, *Technometrics,*
936 *8*(3), 431-444, https://doi.org/10.1080/00401706.1966.10490375.

937 Hayward, T., A. Mantyla (1990), Physical, chemical and biological structure of a coastal eddy near Cape
938 Mendocino, *J. Mar. Res.,* 48(4), 825-850, https://doi.org/10.1357/002224090784988683.
939 Hickey, B.M., N. S. Banas (2009), Why is the northern California Current System so productive?,
940 *Oceanography,* 21(4), 90.
941 Hobday A. A. J., E. C. J. Oliver, A. Sen Gupta, J.A. Benthuysen, M.T. Burrows, M.G. Donat, N.J. Holbrook,
942 P. J. Moore, M.S. Thomsen, T. Wernberg, D.A. Smale (2018), Categorizing and naming marine
943 heatwaves, *Oceanography*, 31(2), 1-13, https://doi.org/10.5670/oceanog.2018.205.
944 Hooff, R. C. W. T. Peterson (2006), Copepod biodiversity as an indicator of changes in ocean and climate
945 conditions of the northern California current ecosystem, *Limnol. Oceanogr.*, *51*(6), 2607-2620,
946 https://doi.org/10.4319/lo.2006.51.6.2607
947 Iguchi, N., T. Ikeda (1995), Growth, metabolism and growth efficiency of a euphausiid crustacean
948 *Euphausia pacifica* in the southern Japan Sea, as influenced by temperature, *J. Plankton*
949 *Res.*, *17*(9), 1757-1769.
950 Jacox, M. G., E. L. Hazen, K. D. Zaba, D. L. Rudnick, C. A. Edwards, A. M. Moore, S. J. Bograd (2016),
951 Impacts of the 2015–2016 El Niño on the California Current System: Early assessment and
952 comparison to past events, *Geophys. Res. Lett.,* 43, 7072–7080,
953 https://doi.org/10.1002/2016GL069716.
954 Jacox, M. G., M.A. Alexander, N. J. Mantua, J. D. Scott, G. Hervieux, R. S. Webb, F. E. Werner (2018a),
955 Forcing of multiyear extreme ocean temperatures that impacted California current living marine
956 resources in 2016, *Bull. Amer. Meteor. Soc.,* 99(1), S27–S33, https://doi.org/10.1175/bams-d-17-
957 0119.1.
958 Jacox, M. G., Edwards, C. A., Hazen, E. L., Bograd, S. J. (2018b), Coastal upwelling revisited: Ekman,
959 Bakun, and improved upwelling indices for the U.S. west coast, *J. Geophys. Res*.,
960 https://doi.org/10.1029/2018JC014187.
961 Jager, T. E. Ravagnan (2015), Parameterising a generic model for the dynamic energy budget of Antarctic
962 krill *Euphausia superba*, *Mar. Ecol. Prog. Ser.,* 519, 115-128.
963 Jones, T., J. K. Parrish, W. T. Peterson, E. P. Bjorkstedt, N.A. Bond, L.T. Balance, V. Bowes, J.M. Hipfner,
964 H.K. Burgess, J. E. Dolliver, K. Lindquist, J. Lindsey, H. M. Nevins, R. R. Robertson, J. Roletto, L.
965 Wilson, T. Joyce, J. Harvey (2018), Massive mortality of a planktivorous seabird in response to a
966 marine heatwave, *Geophys. Res. Lett.*, 45(7), 3193-3202,
967 https://doi.org/10.1002/2017GL076164.

968 JPL MUR MEaSUREs Project (2010), GHRSST Level 4 MUR Global Foundation Sea Surface Temperature
969 Analysis. Ver. 2. PO.DAAC, CA, USA, http://dx.doi.org/10.5067/GHGMR-4FJ01.
970 Ju, S. J., H. K. Kang, W. S. Kim, H. R. Harvey (2009), Comparative lipid dynamics of euphausiids from the
971 Antarctic and Northeast Pacific Oceans, *Mar. Bio.*, *156*(7), 1459-1473,
972 https://doi.org/10.1007/s00227-009-1186-1.
973 Keister, J. E., T. B. Johnson, C. A. Morgan, W.T. Peterson (2005), Biological indicators of the timing and
974 direction of warm-water advection during the 1997/1998 El Niño off the central Oregon coast,
975 USA, *Mar. Ecol. Prog. Ser.*, *295*, 43-48, https://doi.org/10.3354/meps295043.
976 Lamb, J., W. Peterson (2005), Ecological zonation of zooplankton in the COAST study region off central
977 Oregon in June and August 2001 with consideration of retention mechanisms, *J. Geophys. Res*.
978 Oceans, 110(C10).
979 Lasker, R. (1966), Feeding, growth, respiration, and carbon utilization of a euphausiid crustacean, *J. Fish.*
980 *Res. Board Can.*, *23*(9), 1291-1317.
981 Largier, J. L., B. A. Magnell, C. D. Winant (1993), Subtidal circulation over the northern California shelf*, J.*
982 *Geophys. Res.*, 98(C10) 18147-18179, https://doi.org/10.1029/93JC01074.
983 Leising, A. W., I.D. Schroeder, S. J. Bograd, J. Abell, R. Durazo, G. Gaxiola-Castro, E. P. Bjorkstedt, J. Field,
984 K. Sakuma, R. R. Robertson, R. Goericke (2015), State of the California Current 2014-15: Impacts
985 of the Warm-Water "Blob", *Calif. Coop. Oceanic Fish. Invest. Rep*., 56, 31-68.
986 Lilly, L. E., M. D. Ohman (2018), CCE IV: El Niño-related zooplankton variability in the southern California
987 Current System, *Deep Sea Res. Pt. I, 140*, 36-51.
988 Lindley S. T., C. B. Grimes, M.S. Mohr, W. Peterson, J. Stein, J. T. Anderson, L. W. Botsford, D. L Bottom,
989 C. A. Busack, T. K. Collier, J. Ferguson, J. C. Garza, A. M. Grover, D. G. Hankin, R. G. Kope, P.W.
990 Lawson, A. Low, R. B. MacFarlane, K. Moore, M. Palmer-Zwahlen, F. B. Schwing, J. Smith, C.
991 Tracy, R. Webb, B. K. Wells, T. H. Williams (2009), What Caused the Sacramento River Fall
992 Chinook Stock Collapse?, Report to the Pacific Fishery Management Council.
993 Lindsey, B. J., H. P. Batchelder (2011), Cross-shelf distribution of Euphausia pacifica in the Oregon coastal
994 upwelling zone: field evaluation of a differential transport hypothesis, J. *Plankton Res*., 33(11),
995 1666-1678.
996 Logerwell, E. A., N. Mantua, P.W. Lawson, R. C. Francis, V. N. Agostini (2003), Tracking environmental
997 processes in the coastal zone for understanding and predicting Oregon coho (Oncorhynchus
998 kisutch) marine survival, *Fish. Oceanogr.*, *12*(6), 554-568.

Lovvorn, J. R. (2010), Modeling profitability for the smallest marine endotherms: auklets foraging within pelagic prey patches, *Aquat. Biol*., 8(3), pp.203-219.

Mackas, D., M. Galbraith (2002), Zooplankton community composition along the inner portion of Line P during the 1997-1998 El Niño Event, *Prog. Oceanogr.,* 54(1), 423-437, https://doi.org/10.1016/S0079-6611(02)00062-9.

Mangel, M., D. Ludwig (1992), Definition and evaluation of the fitness of behavioral and developmental programs, *Annu. Rev. Ecol. Evol. Syst.*, 23(1), 507-536.

Marinovic, B., M. Mangel (1999), Krill can shrink as an ecological adaptation to temporarily unfavorable environments, *Ecol. Lett.,* 2, 338-343.

Marinovic, B. B., D.A. Croll, N. Gong, S.R. Benson, F. P. Chavez (2002), Effects of the 1997-1999 El Niño and La Niña events on zooplankton abundance and euphausiid community composition within the Monterey Bay coastal upwelling system, *Prog. Oceanogr.,* 54, 265-277, https://doi.org/10.1016/S0079-6611(02)00053-8.

McCabe, R. M., B. M. Hickey, R. M. Kudela, K. A. Lefebvre, N. G. Adams, B. D. Bill, F. Gulland, R. E. Thomson, W. P. Cochlan, V. L. Trainer (2016), An unprecedented coastwide toxic algal bloom linked to anomalous ocean conditions, *Geophys. Res. Lett.,* 43(10), 366-376, https://doi.org/10.1002/2016GL070023.

McClatchie, S., R. Goericke, A. Leising, T. D. Auth, E. Bjorkstedt, R.R. Robertson, R. D. Brodeur, X. Du, E. A. Daly, C. A. Morgan, F. P. Chavez, A. J. Debich, J. Hildebrand, J. Field, K. Sakuma, M. G. Jacox, M. Kahru, R. Kudela, C. Andserson, J. Largier, B.E. Lavaniegos, J. Gomez-Valdes, S. P. A. Jimenez-Rosenberg, R. McCabe, S. R. Melin, M. D. Ohman, L. M. Sala, B. Peterson, J. Fisher, I. D. Shroeder, S. J. Bograd, E. L. Hazen, S. R. Schneider, R. T. Golightly, R. M. Suryan, A. J. Gladics, S. Loredo, J. M. Porquez, A. R. Thompson, E. D. Weber, W. Watson, V. Trainer, P. Warzybok, R. Bradley, J. Jahncke (2016), State of the California Current 2015-16: Comparisons with the 1997-98 El Niño, *Calif. Coop. Oceanic Fish. Invest. Rep*., 57, 5-61.

McLaskey, A. K., J. E. Keister, L. Yebra (2020), Individual growth rate (IGR) and aminoacyl-tRNA synthetases (AARS) activity as individual-based indicators of growth rate of North Pacific krill, *Euphausia pacifica*, *J. Exp. Mar. Biol. Ecol*., *527*, 151360.

McPhaden, M. J. (2015), Playing hide and seek with El Niño, *Nat. Clim. Change*, 5, 791-795, https://doi.org/10.1038/nclimate2775.

1029 Nicol, S., M. Stolp, T. Cochran, P. Geijsel, J. Marshall (1992), Growth and shrinkage of Antarctic krill
1030 *Euphausia superba* from the Indian Ocean sector of the Southern Ocean during summer. *Mar.*
1031 *Ecol. Prog. Ser., Oldendorf*, *89*(2), 175-181.
1032 O'Connor, M. I., J.F. Bruno, S. D. Gaines,B. S. Halpern, S. E. Lester, B. P. Kinlan, J. M. Weiss (2007),
1033 Temperature control of larval dispersal and the implications for marine ecology, evolution, and
1034 conservation, *PNAS*, *104*(4), 1266-1271.
1035 Ohman, M. D. (1984), Omnivory by *Euphausia pacifica*: The role of copepod prey, *Mar. Ecol. Prog. Ser.*
1036 *Oldendorf*, *19*(1), 125-131.
1037 Ohman, M.D., (1986), Predator-limited population growth of the copepod *Pseudocalanus sp*., *J. Plankton*
1038 *Res.*, 8(4), 673-713.
1039 Oksanen, J., F. G. Blanchet, R. Kindt, P. Legendre, P. R. Minchin, R. B. O'Hara, G. L. Simpson, P. Solymos,
1040 M. H. Stevens, H. Wagner, M. H. Oksanen (2013), Package 'vegan'. Community ecology package,
1041 version 2(9).
1042 Oliver, E.C., M.G. Donat, M.T. Burrows, P.J. Moore, D.A. Smale, L.V. Alexander, J.A. Benthuysen, M. Feng,
1043 A.S. Gupta, A.J. Hobday, and N.J. Holbrook (2018), Longer and more frequent marine heatwaves
1044 over the past century, *Nat. Commun.*, *9*(1), 1324, https://doi.org/10.1038/s41467-018-03732-9.
1045 Paradis, A. R., P. Pepin, J. A. Brown (1996), Vulnerability of fish eggs and larvae to predation: review of
1046 the influence of the relative size of prey and predator, *Can. J. Fish. Aquat. Sci.*, 53(6), 1226-1235.
1047 Peterson, I., J. S. Wroblewski (1984), Mortality rate of fishes in the pelagic ecosystem, *Can. J. Fish. Aquat.*
1048 *Sci.*, *41*(7), 1117-1120, https://doi.org/10.1139/f84-131.
1049 Peterson, W., M. Robert, N. Bond, (2015), The warm blob continues to dominate the ecosystem of the
1050 northern California current, *PICES Press*, *23*(2), 44.
1051 Peterson, W. T., J. L. Fisher, P. T. Strub, X. Du, C. Risien, J. Peterson, C. T. Shaw (2017), The pelagic
1052 ecosystem in the northern California Current off Oregon during the 2014-2016 warm anomalies
1053 within the context of the past 20 years, *J. Geophys. Res. Oceans*, 122, 7267-7290,
1054 https://doi.org/10.1002/2017JC012952.
1055 Pinchuk, A., R. Hopcroft (2007), Seasonal variations in the growth rates of euphausiids (*Thysanoessa*
1056 *inermis*, *T. spinifera*, and *Euphausia pacifica*) from the northern Gulf of Alaska, *Mar. Biol.,* 151,
1057 257-269, https://doi.org/10.1007/s00227-006-0483-1.
1058 Pinheiro J., D. Bates, S. DebRoy, D. Sarkar, R Core Team (2018), nlme: Linear and Nonlinear Mixed Effects
1059 Models, R package version 3.1-137, https://CRAN.R-project.org/package=nlme.

1060 Poleck, T. P. C. J. Denys (1982), Effect of temperature on the molting, growth and maturation of the
1061 Antarctic krill *Euphausia superba* (Crustacea: Euphausiacea) under laboratory conditions, *Mar.*
1062 *Biol.*, 70(3), 255-265.
1063 R Core Team (2018), R: A language and environment for statistical computing. R Foundation for
1064 Statistical Computing, Vienna, Austria, http://www.R-project.org/.
1065 Ressler, P., R. D. Brodeur, W. T. Peterson (2005), The spatial distribution of euphausiid aggregations in
1066 the Northern California Current during August 2000, *Deep Sea Res. Pt. II*, 52, 89-108,
1067 https://doi.org/10.1016/j.dsr2.2004.09.032.
1068 Ross, R. M. (1979), Carbon and nitrogen budgets over the life of *Euphausia pacifica*, PhD. Thesis,
1069 University of Washington, Seattle, WA.
1070 Ross, R. M. (1981), Laboratory culture and development of *Euphausia pacifica*, *Limnol. Oceanogr*., 26(2)
1071 235-246, https://doi.org/10.4319/lo.1981.26.2.0235.
1072 Ross, R.M. (1982a), Energetics of *Euphausia pacifica*. I. Effects of body carbon and nitrogen and
1073 temperature on measured and predicted production, *Mar. Bio.*, 68(1), 1-13.
1074 Ross, R. M. (1982b), Energetics of *Euphausia pacifica*. II. Complete carbon and nitrogen budgets at 8 and
1075 12 C throughout the life span, *Mar. Bio.*, *68*(1), 15-23.
1076 Ruzicka, J. J., R. D. Brodeur, R. L. Emmett, J. H. Steele, J. E. Zamon, C. A. Morgan, A. C. Thomas, T. C.
1077 Wainwright (2012), Interannual variability in the Northern California Current food web
1078 structure: Changes in energy flow pathways and the role of forage fish, euphausiids, and
1079 jellyfish, *Prog. Ocean.,* 102, 19-41, https://doi.org/10.1016/j.pocean.2012.02.002.
1080 Sakuma, K. M., J. C. Field, N. J. Mantua, S. Ralston (2016), Anomalous epipelagic micronekton
1081 assemblage patterns in the neritic waters of the California Current in spring 2015 during a
1082 period of extreme ocean conditions, *Calif. Coop. Oceanic Fish. Invest. Rep*., 57, 163-183.
1083 Santora, J. A., W. J. Sydeman, I. D. Schroeder, B. K. Wells, J. C. Field (2011), Mesoscale structure and
1084 oceanographic determinants of krill hotspots in the California Current: Implications for trophic
1085 transfer and conservation, *Prog. Ocean.,* 91, 397-409,
1086 https://doi.org/10.1016/j.pocean.2011.04.002.
1087 Santora J. A., J. C. Field, I. D. Schroeder, K. M. Sakuma, B. K. Wells, W. J. Sydeman (2012), Spatial ecology
1088 of krill, micronecktон and top predators in the central California Current: Implications for
1089 defining ecologically important areas, *Prog. Ocean.,* 106, 154-174,
1090 https://doi.org/10.1016/j.pocean.2012.08.005.

1091 Santora, J. A., N. J. Mantua, I. D. Schroeder, J. C. Field, E. L. Hazen, S. J. Bograd, W. J. Sydeman, B. K.
1092 Wells, J. Calambokidis, L. Saez, D. Lawson (2020), Habitat compression and ecosystem shifts as
1093 potential links between marine heatwave and record whale entanglements, *Nat.*
1094 *Commun.*, *11*(1), 1-12.
1095 Schoenherr, J. R. (1991), Blue whales feeding on high concentrations of euphausiids around Monterey
1096 Submarine Canyon, *Can. J. of Zool.*, 69(3), 583-594, https://doi.org/10.1139/z91-088.
1097 Schroeder, I. D., B. A. Black, W. J. Sydeman, S. J. Bograd, E. L. Hazen, J. A. Santora, B. K. Wells (2013), The
1098 North Pacific High and wintertime pre-conditioning of California current productivity, *Geophys.*
1099 *Res. Lett.*, *40*(3), 541-546.
1100 Siegel, V. (2000) Krill (Euphausiacea) life history and aspects of population dynamics, *Can. J. Fish. Aquat.*
1101 *Sci*, 57(S3), 130-150.
1102 Shaw, C. T., W. T. Peterson, L. R. Feinberg (2010), Growth of *Euphausia pacifica* in the upwelling zone off
1103 the Oregon coast, *Deep Sea Res. Pt. II,* 57(7-8), 584-93,
1104 https://doi.org/10.1016/j.dsr2.2009.10.008.
1105 Shin, H. C., S. Nicol (2002), Using the relationship between eye diameter and body length to detect the
1106 effects of long-term starvation on Antarctic krill *Euphausia superba*, *Mar. Ecol. Prog. Ser*., 239,
1107 157-167.
1108 Smiles, M. C., W. G. Pearcy (1971), Size structure and growth rate of *Euphausia pacifica* off the Oregon
1109 coast, *Fish. Bull.,* 69(1) 79-86.
1110 Smith, P. (1985), A case history of an anti-El Niño to El Niño transition on plankton and nekton
1111 distribution and abundances. In: Wooster WS, Fluharty DL (Eds.), El Niño North: Niño effects in
1112 the eastern subarctic Pacifica Ocean, Washington Sea Grant Program, Seattle, 121-142.
1113 Stuart, V., S. C. Pillar (1990), Diel grazing patterns of all ontogenetic stages of *Euphausia lucens* and in
1114 situ predation rates on copepods in the southern Benguela upwelling region, *Mar. Ecol. Prog.*
1115 *Ser.*, 227-241.
1116 Strub, P., C. James (2000), Altimeter-derived variability of surface velocities in the California Current
1117 System: 2. Seasonal circulation and eddy statistics, *Deep Sea Res. Pt. II,* 47, 831-870,
1118 https://doi.org/10.1016/S0967-0645(99)00129-0.
1119 Sydeman, W. J., R. W. Bradley, P. Warzybok, C. L. Abraham, J. Jahncke, K. D. Hyrenbach, V. Kousky, J. M.
1120 Hipfner, M. D. Ohman (2006), Planktivorous auklet *Ptychoramphus aleuticus* responses to ocean
1121 climate, 2005: Unusual atmospheric blocking?, *Geophys. Res. Lett.,* 33, L22S09,
1122 https://doi.org/10.1029/2006GL026736.

Sydeman, W. J., J. A. Santora, S. A. Thompson, B. Marinovic, E. Di Lorenzo (2013), Increasing variance in North Pacific climate relates to unprecedented ecosystem variability off California, *Glob. Chang. Biol.,* 19, 1662-1675, https://doi.org/10.1111/gcb.12165.

Tanasichuk, R. W. (1998), Interannual variations in the population biology and productivity of *Euphausia pacifica* in Barkley Sound, Canada, with special reference to the 1992 and 1993 warm ocean years, *Mar. Ecol. Prog. Ser.*, *173*, https://doi.org/10.3354/meps173163.

Tanasichuk, R. W. (2002), Implications of interannual variability in euphausiid population biology for fish production along the southwest coast of Vancouver Island: a synthesis, *Fish. Ocean*., 11(1), 18-30, https://doi.org/10.1046/j.1365-2419.2002.00185.x.

Theilacker, G. H., N. C. H. Lo, A. W. Townsend (1993), An immunochemical approach to quantifying predation by euphausiids on the early stages of anchovy, *Mar. Ecol. Prog. Ser*., 35-50.

Wei, T., S. Viliam (2017), R package "corrplot": Visualization of a Correlation Matrix (Version 0.84).

Wells, B. K., J. A. Santora, J. C. Field, R. B. MacFarlane, B. B. Marinovic, W. J. Sydeman (2012), Population dynamics of Chinook salmon *Oncorhynchus tshawytscha* relative to prey availability in the central California coastal region, *Mar. Ecol. Prog. Ser*., 457, 125-137.

Wells, B. K., I. D. Schroeder, J. A. Santora, E. L. Hazen, S. J. Bograd, E. P. Bjorkstedt, V. J. Loeb, S. Mcclatchie, E. D. Weber, W. Watson, A. R. Thompson, W. T. Peterson, R. D. Brodeur, J. Harding, J. Field, K. Sakuma, S. Hayes, N. Mantua, W. Sydeman, M. Losekoot, S. A. Thompson, J. Largier, S. Y. Kim, F. P. Chavez, C. Barceló, P. Warzybok, , R. Bradley, J. Jahncke, R. Goericke, G. S. Campbell, J. Hildebrand, S. R. Melin, R. L. Long, J. Gomez-Valdez, B. Lavaniegos, G. Gaxiola-Castro, R. T. Golightly, S. R. Schneider, N. Lo, R. M. Suryan, A. J. Gladics, C. A. Horton, J. Fisher, C. Morgan, J. Peterson, E. A. Daly, T. D. Auth, J. Abell (2013), State of the California Current 2012-13: No such thing as an" average" year. *California Cooperative Oceanic Fisheries Investigations Reports*, *54*, 37-71.

Wells, B. K., I. D. Schroeder, S. J. Bograd, E. L. Hazen, M. G. Jacox, A. Leising, N. Mantua, J. A. Santora, J. Fisher, W. T. Peterson, E. Bjorkstedt, R. R. Robertson, F. P. Chavez, R. Goericke, R. Kudela, C. Anderson, B. E. Lavaniegos, J. Gomez-Valdes, R. D. Brodeur, E. A. Daly, C. A. Morgan, T. D. Auth, J. C. Field, K. Sakuma, S. McClatchie, A. R. Thompson, E. D. Weber, W. Watson, R. M. Suryan, J. Parrish, J. Dolliver, S. Loredo, J. M. Porquez, J. E. Zamon, S. R. Schneider, R. T. Golightly, P. Warzybok, R. Bradley, J. Jahncke, W. Sydeman, S. R. Melin, J. Hildebrand, A. J. Debich, B. Thayre (2017), State of the California Current 2016–2017: still anything but ‘‘normal’’ in the north, *Calif. Coop. Oceanic Fish. Invest. Rep*., 58, 1–55.

1155 Wolf, S. G., M. A. Snyder, W. J. Sydeman, D. F. Doak, D. A Croll (2010), Predicting population
1156 consequences of ocean climate change for an ecosystem sentinel, the seabird Cassin's auklet.
1157 *Glob. Chang. Biol*., 16(7), 1923-1935.
1158 Wood, S. N. (2017), *Generalized additive models: an introduction with R*, Chapman and Hall/CRC.
1159 Zuur, A., E.N. Ieno, N. Walker, A.A. Saveliev, G.M. Smith (2009), *Mixed effects models and extensions in*
1160 *ecology with R*, Springer, New York.
1161 Zuur, A.F., E.N Ieno, C.S. Elphick, (2010), A protocol for data exploration to avoid common statistical
1162 problems, *Methods Ecol. Evol.*, *1*(1), 3-14.